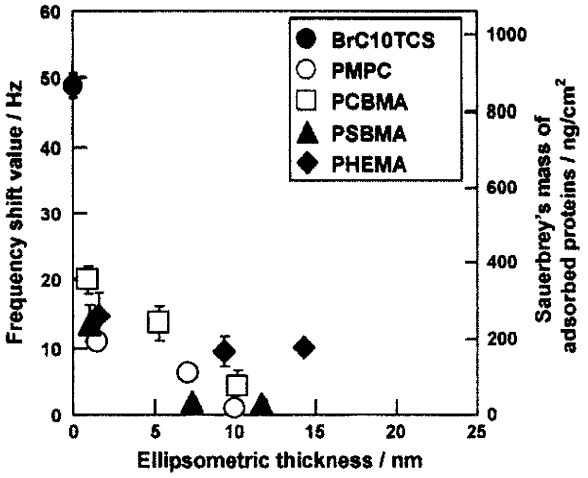

Fig. 7. The amount of proteins adsorbed relative to 100% fetal bovine serum (FBS) on the BrC10TCS-immobilized substrate (closed circle), poly(MPC)-grafted substrate (open circles), poly(CBMA)-grafted substrate (open squares), poly(SBMA)-grafted substrate (closed triangles), and poly(HEMA)-grafted substrate (closed diamonds).

wafer surface. The grafted polymer chains in the polymer brush structure probably completely span the substrate without gaps, even for thin grafted polymer layers. Thus, the unreacted bromoisobutyryl group at the silicon wafer surface would probably not affect the surface properties of thin polymer-grafted substrates. Grafted polymer chains with low molecular weight are thought to be less mobile. The terminal groups at the grafted polymer chains spanned the outermost surface of the polymer-grafted substrates. Thus, a relatively hydrophobic environment was observed on the surface of the thin polymer-grafted substrates.

In a previous study on the adsorption of proteins on the polymer brush layer, the amount of adsorbed proteins strongly depended on both the polymerization degree and graft density in the polymer brush layer; the amount of adsorbed protein reached 5 ng/cm^2, which is approximately 300 times less than the amount of conventional materials, including polystyrene for tissue culture, glass, etc. We could not uniformly compare the resistance to protein adsorption on several kinds of polymer brush layers among different proteins because protein adsorption was determined for various polymers in different apparatus and under varying experimental conditions of temperature, protein concentration, protein type, and pH of the protein solution. To elucidate the effect of the monomer moiety on protein adsorption, the interaction between the proteins and surface should be analyzed under identical experimental conditions.

Prior to the determination of protein adsorption on the polymer-grafted substrates, we characterized the surface physicochemical properties of the polymer-grafted layers formed on the gold substrates, and compared with those on the silicon wafers. The graft density of polymer chains in the polymer brush layers formed on gold and silicon was almost the same, and there was little difference in the static water contact angles for the polymer-grafted substrates between gold and silicon. These results indicated that the two types of the polymer-grafted surface have the same properties. The amount of protein adsorbed on the polymer-grafted substrates was quantified using QCM-D relative to 100% FBS. The amount of adsorbed proteins on the polymer-grafted substrates was plotted against the thickness of the polymer layer determined using an ellipsometer (Fig. 7). Consistent with previous reports, the amount of adsorbed proteins on each polymer-grafted substrate gradually decreased with increase in the thickness of the polymer layer in the range of 1–15 nm. The cause for the effect of polymer layer thickness on protein adsorption has yet to be clarified; nevertheless, the terminal group at the grafted polymer chains probably plays an important role in protein adsorption behavior at the surface of polymer-grafted substrates, as indicated by the wettability values. Protein adsorption was dramatically reduced on the surface of three kinds of zwitterionic polymer-grafted substrates with an approximate thickness of 10 nm (poly(MPC)-grafted substrate, 17 ng/cm^2; poly(SBMA)-grafted substrate, 31 ng/cm^2; and poly(CBMA)-grafted substrate, 79 ng/cm^2), when compared with the protein adsorption on the initiator-immobilized substrate (870 ng/cm^2). However, the amount of adsorbed proteins on the surface of a nonionic polymer-grafted substrate (i.e., poly(HEMA)) with an approximate thickness of 15 nm was relatively high (180 ng/cm^2). These results suggest that protein adsorption depends on the structure of the monomer unit. For polymer-grafted substrates with a thickness of a few nanometers, the amount of proteins adsorbed was slightly higher (200–300 ng/cm^2) than that of thicker polymer-grafted substrates irrespective of the structure of the monomer unit. Interestingly, the amount of protein adsorbed onto thin poly(MPC)-grafted substrates was nearly equivalent to that adsorbed onto other thin polymer-grafted substrates even though the surface coverage of the grafted polymer was relatively low, as mentioned above. This result emphasizes the effect of the terminal group at the surface of the grafted polymer chains with a small molecular weight, rather than that of the unreacted bromoisobutyryl group at the silicon wafer surface, on the kinds of surface properties acquired by the grafted polymer chains. We are currently investigating protein adsorption behavior on polymer brush layers composed of hydrophilic monomer moieties and hope to report these findings in the near future.

4. Conclusion

We synthesized four kinds of polymer-grafted substrates, namely, poly(MPC), poly(SBMA), poly(CBMA), and poly(HEMA) brush structures, with thickness ranging from 1 to 20 nm, on silicon wafers using the SI-ATRP method with high and defined graft density. The graft density and surface coverage with the polymer chains depended on the chemical structure of the monomer units; these parameters were high enough to enable the formation of dense polymer brush structures. Moreover, only slight differences were observed in the AFM height images of the polymer-grafted substrates of nearly equivalent thickness. Nevertheless, the wettability by water increased with increasing thickness of the grafted polymer layers, thereby indicating that the terminal group at the grafted polymer chain surface affects the surface properties. Protein adsorption was effectively suppressed on the surface of thick zwitterionic polymer-grafted substrates when compared with that on nonionic polymer-grafted substrates, thereby indicating that the structure of the monomer unit in the grafted polymer layers also strongly affects the surface properties of the polymer-grafted substrates. On the basis of the similarities and differences between the surface structure characteristics and protein adsorption among different monomer units forming the polymer brush layers with well-characterized surface structures, we determined that the chemical structure is a key factor that affects biocompatibility. We believe that nanostructure-controlled polymer brush layers composed of hydrophilic monomer units would be ideal surface structures to help elucidate the relationship among surface structure, surface properties, and protein adsorption behavior and would be useful for designing novel biomedical devices.

References

[1] H. Chen, L. Yuan, W. Song, Z. Wu, D. Li, Prog. Polym. Sci. 33 (2008) 1059–1087.
[2] K. Ishihara, M. Takai, J. R. Soc. Interface 6 (2009) S279–S291.

[3] A.S. Kohler, P.J. Parks, D.L. Mooradian, G.H.R. Rao, L.T. Furcht, J. Biomed. Mater. Res. 32 (1996) 237–242.
[4] K. Ishihara, T. Ueda, N. Nakabayashi, Polym. J. 22 (1990) 355–360.
[5] S. Chen, J. Zheng, L. Li, S. Jiang, J. Am. Chem. Soc. 127 (2005) 14473–14478.
[6] K. Sugiyama, K. Ohga, H. Aoki, Macromol. Chem. Phys. 196 (1995) 1907–1916.
[7] L. Ruiz, J.G. Hilborn, D. Leonard, H.J. Mathieu, Biomaterials 19 (1998) 987–998.
[8] K. Ishihara, H. Nomura, T. Mihara, K. Kurita, Y. Iwasaki, N. Nakabayashi, J. Biomed. Mater. Res. 39 (1998) 323–330.
[9] K. Ishihara, N.P. Ziats, B.P. Tierney, N. Nakabayashi, J.M. Anderson, J. Biomed. Mater. Res. 25 (1991) 1397–1407.
[10] K. Ishihara, H. Oshida, Y. Endo, T. Ueda, A. Watanabe, N. Nakabayashi, J. Biomed. Mater. Res. 26 (1992) 1543–1552.
[11] A.L. Lewis, Colloids Surf. 18 (2000) 261–275.
[12] K. Sugiyama, K. Shiraishi, K. Okada, O. Matsuo, Polym. J. 31 (1999) 883–886.
[13] Y. Inoue, J. Watanabe, K. Ishihara, J. Colloid Interface Sci. 274 (2004) 465–471.
[14] Y. Inoue, J. Watanabe, M. Takai, K. Ishihara, J. Biomater. Sci. Polym. Ed. 15 (2004) 1153–1166.
[15] Y. Inoue, J. Watanabe, M. Takai, S. Yusa, K. Ishihara, J. Polym. Sci. Part A: Polym. Chem. 43 (2005) 6073–6083.
[16] Y. Goto, R. Matsuno, T. Konno, M. Takai, K. Ishihara, Biomacromolecules 9 (2008) 828–833.
[17] M. Kyomoto, T. Moro, T. Konno, H. Takadama, N. Yamasaki, H. Kawaguchi, Y. Takatori, K. Nakamura, K. Ishihara, J. Biomed. Meter. Res. 82 (2007) 10–17.
[18] T. Goda, T. Konno, M. Takai, T. Moro, K. Ishihara, Biomaterials 27 (2006) 5151–5160.
[19] M. Kyomoto, T. Moro, Y. Takatori, H. Kawaguchi, K. Nakamura, K. Ishihara, Biomaterials 31 (2010) 1017–1024.
[20] J. Pyun, T. Kowalewski, K. Matyjaszewski, Macromol. Rapid Commun. 24 (2003) 1043–1059.
[21] C. Yoshikawa, A. Goto, Y. Tsujii, T. Fukuda, T. Kimura, K. Yamamoto, A. Kishida, Macromolecules 39 (2006) 2284–2290.
[22] B.S. Lee, Y.S. Chi, K.B. Lee, Y.G. Kim, I.S. Choi, Biomacromolecules 8 (2007) 3922–3929.
[23] W. Feng, S. Zhu, K. Ishihara, J.L. Brash, Biointerphases 1 (2006) 50–60.
[24] Z. Wu, H. Chen, X. Liu, Y. Zhang, D. Li, H. Huang, Langmuir 25 (2009) 2900–2906.
[25] M. Chen, W.H. Briscoe, S.P. Armes, J. Klein, Science 323 (2009) 1698–1701.
[26] W. Feng, J.L. Brash, S. Zhu, Biomaterials 27 (2006) 847–855.
[27] R. Iwata, P. Suk-In, V.P. Hoven, A. Takahara, K. Akiyoshi, Y. Iwasaki, Biomacromolecules 5 (2004) 2308–2314.
[28] K. Kitano, Y. Inoue, R. Matsuno, M. Takai, K. Ishihara, Colloids Surf. B: Biointerfaces 74 (2009) 350–357.
[29] C.R. Emmenegger, E. Brynda, T. Riedel, Z. Sedlakova, M. Houska, A.B. Alles, Langmuir 25 (2009) 6328–6333.
[30] Z. Zhang, S. Chen, Y. Chang, S. Jiang, J. Phys. Chem. B 110 (2006) 10799–10804.
[31] Y. Chang, S.C. Liao, A. Higuchi, R.C. Ruaan, C.W. Chu, W.Y. Chen, Langmuir 24 (2008) 5453–5458.
[32] G. Li, G. Cheng, H. Xue, S. Chen, F. Zhang, S. Jiang, Biomaterials 29 (2008) 4592–4597.
[33] P.S. Liu, Q. Chen, X. Liu, B. Yuan, S.S. Wu, J. Shen, S.C. Lin, Biomacromolecules 10 (2009) 2809–2816.
[34] Z. Zhang, S. Chen, S. Jiang, Biomacromolecules 7 (2006) 3311–3315.
[35] Z. Zhang, H. Vaisocherová, G. Cheng, W. Yang, H. Xue, S. Jiang, Biomacromolecules 9 (2008) 2686–2692.
[36] G. Cheng, H. Xue, Z. Zhang, S. Chen, S. Jiang, Angew. Chem. Int. Ed. 47 (2008) 8831–8834.
[37] H. Vaisocherová, W. Yang, Z. Zhang, Z. Cao, G. Cheng, M. Piliarik, J. Homola, S. Jiang, Anal. Chem. 80 (2008) 7894–7901.
[38] Z. Zhang, G. Cheng, L.R. Carr, H. Vaisocherová, S. Chen, S. Jiang, Biomaterials 29 (2008) 4719–4725.
[39] H. Vaisocherová, Z. Zhang, W. Yang, Z. Cao, G. Cheng, A.D. Taylor, M. Piliarik, J. Homola, S. Jiang, Biosens. Bioelectron. 24 (2009) 1924–1930.
[40] Z. Zhang, M. Zhang, S. Chen, T.A. Horbett, B.D. Ratner, S. Jiang, Biomaterials 29 (2008) 4285–4291.
[41] T. Morisaku, J. Watanabe, T. Konno, M. Takai, K. Ishihara, Polymer 49 (2008) 4652–4657.
[42] K. Matyjaszewski, P.J. Miller, N. Shukla, B. Immaraporn, A. Gelman, B.B. Luokala, T.M. Siclovan, G. Kickelbick, T. Vallant, H. Hoffmann, T. Pakula, Macromolecules 32 (1999) 8716–8724.
[43] M. Husseman, E.E. Malmstrom, M. McNamara, M. Mate, D. Mecerreyes, D.G. Benoit, J.L. Hedrick, P. Mansky, E. Huang, T.P. Russell, C.J. Hawker, Macromolecules 32 (1999) 1424–1431.
[44] K. Yamamoto, Y. Miwa, H. Tanaka, M. Sakaguchi, S. Shimada, J. Polym. Sci. A: Polym. Chem. 40 (2002) 3350–3359.
[45] A. Dolatshahi-Pirouz, K. Rechendorff, M.B. Hovgaard, M. Foss, J. Chevallier, F. Besenbacher, Colloids Surf. B: Biointerfaces 66 (2008) 53–59.
[46] A.G. Hemmersam, M. Foss, J. Chevallier, F. Besenbacher, Colloids Surf. B: Biointerfaces 43 (2005) 208–215.
[47] D.M. Jones, A.A. Brown, W.T.S. Huck, Langmuir 18 (2002) 1265–1269.
[48] W. Feng, J. Brash, S. Zhu, J. Polym. Sci. Part A: Polym. Chem. 42 (2004) 2931–2942.
[49] A.B. Lowe, C.L. McCormick, Chem. Rev. 102 (2002) 4177–4189.
[50] W. Yang, H. Xue, W. Li, J. Zhang, S. Jiang, Langmuir 25 (2009) 11911–11916.
[51] W. Yang, S. Chen, G. Cheng, H. Vaisocherová, H. Xue, W. Li, J. Zhang, S. Jiang, Langmuir 24 (2008) 9211–9214.
[52] O. Azzaroni, A.A. Brown, W.T.S. Huck, Angew. Chem. Int. Ed. 45 (2006) 1770–1774.
[53] N. Cheng, A.A. Brown, O. Azzaroni, W.T.S. Huck, Macromolecules 41 (2008) 6317–6321.
[54] Z. Zhang, T. Chao, S. Chen, S. Jiang, Langmuir 22 (2006) 10072–10077.
[55] M. Ejaz, K. Ohno, Y. Tsujii, T. Fukuda, Macromolecules 33 (2000) 2870–2874.
[56] Y. Tsujii, K. Ohno, S. Yamamoto, A. Goto, T. Fukuda, Adv. Polym. Sci. 197 (2006) 1–45.
[57] M. Kobayashi, Y. Terayama, N. Hosaka, M. Kaido, A. Suzuki, N. Yamada, N. Torikai, K. Ishihara, A. Takahara, Soft Matter 3 (2007) 740–746.

Osteoarthritis and Cartilage 18 (2010) 1174–1182

Osteoarthritis and Cartilage

OARSI OSTEOARTHRITIS RESEARCH SOCIETY INTERNATIONAL

Surface grafting of biocompatible phospholipid polymer MPC provides wear resistance of tibial polyethylene insert in artificial knee joints

T. Moro †, Y. Takatori †, M. Kyomoto †, K. Ishihara ‡, K. Saiga †, K. Nakamura §, H. Kawaguchi §*

† *Department of Science for Joint Reconstruction, The University of Tokyo, Hongo 7-3-1, Bunkyo, Tokyo 113-0033, Japan*
‡ *Department of Materials Engineering, The University of Tokyo, Hongo 7-3-1, Bunkyo, Tokyo 113-0033, Japan*
§ *Department of Sensory & Motor System Medicine, The University of Tokyo, Hongo 7-3-1, Bunkyo, Tokyo 113-0033, Japan*

ARTICLE INFO

Article history:
Received 20 January 2010
Accepted 29 May 2010

Keywords:
Artificial knee joint
Arthroplasty
Polyethylene
Wear
Loosening

SUMMARY

Objective: Aseptic loosening of artificial knee joints induced by wear particles from a tibial polyethylene (PE) insert is a serious problem limiting their longevity. This study investigated the effects of grafting with our original biocompatible phospholipid polymer 2-methacryloyloxyethyl phosphorylcholine (MPC) on the insert surface.

Methods: The hydrophilicity of the PE surface was determined by the contact angle of a water droplet, and the friction torque was measured against a cobalt–chromium alloy component. The wear amount was compared among PE inserts with or without cross-linking and MPC grafting during 5×10^6 cycles of loading in a knee joint simulator. The surfaces of the insert and the wear particles in the lubricant were subjected to electron and laser microscopic analyses. The mechanical properties of the inserts were evaluated by the small punch test.

Results: The MPC grafting increased hydrophilicity and decreased friction torque. In the simulator experiment, the wear of the tibial insert was significantly suppressed in the cross-linked PE (CLPE) insert, and even more dramatically decreased in the MPC-grafted CLPE insert, as compared to that in the non-cross-linked PE insert. Surface analyses confirmed the wear resistance by the cross-linking, and further by the MPC grafting. The particle size distribution was not affected by cross-linking or MPC grafting. The mechanical properties of the insert material remained unchanged during the loading regardless of the cross-linking or grafting.

Conclusion: Surface grafting with MPC polymer furnished the PE insert with wear resistance in an artificial knee joint through increased hydrophilicity and decreased friction torque.

Introduction

Total knee arthroplasty (TKA) and total hip arthroplasty (THA) are effective treatments for patients with severe arthritis of the joints. Recent surveys revealed that the number of surgical procedures are growing faster than ever due to the expansion of the elderly population[1,2]. Despite improvement in the implant design of the prostheses and the surgical technique employed, the aseptic loosening caused by periprosthetic osteolysis is a serious problem limiting their survivorship and clinical success[2,3]. The osteolysis is triggered by the host inflammatory responses to the polyethylene (PE) wear particles originating from the interface[4,5], which induce the phagocytosis by macrophages and the following secretion of bone resorptive cytokines[6]. Hence, aiming at reduction of the PE wear particles, various trials have been performed. Of these, highly cross-linked PE (CLPE) achieved the most successful reduction in the wear rate compared with the conventional PE[7–13], and is now widely used in clinical settings[14,15].

In natural synovial joints under physiological conditions, fluid film lubrication by the intermediate hydrated layer is known to be essential for the smooth motion[16,17], and a nanometer-scaled phospholipid layer which covers the joint cartilage surface provides hydrophilicity and works as an effective boundary lubricant[18]. Hence, grafting a phospholipid-like layer on the surface may realize ideal hydrophilicity and lubricity resembling the physiological joint surface. The 2-methacryloyloxyethyl phosphorylcholine (MPC) polymer is our original biocompatible polymer whose side chain is composed of phosphorylcholine mimicking the neutral phospholipids of biomembranes[19] [Fig. 1(A)]. The MPC grafting onto the surface of medical devices has already been shown to suppress

* Address correspondence and reprint requests to: Hiroshi Kawaguchi, Sensory & Motor System Medicine, Faculty of Medicine, University of Tokyo, Hongo 7-3-1, Bunkyo, Tokyo 113-8655, Japan. Tel: 81-3-3815-5411x30473; Fax: 81-3-3818-4082.
E-mail address: kawaguchi-ort@h.u-tokyo.ac.jp (H. Kawaguchi).

1063-4584/$ – see front matter
doi:10.1016/j.joca.2010.05.019

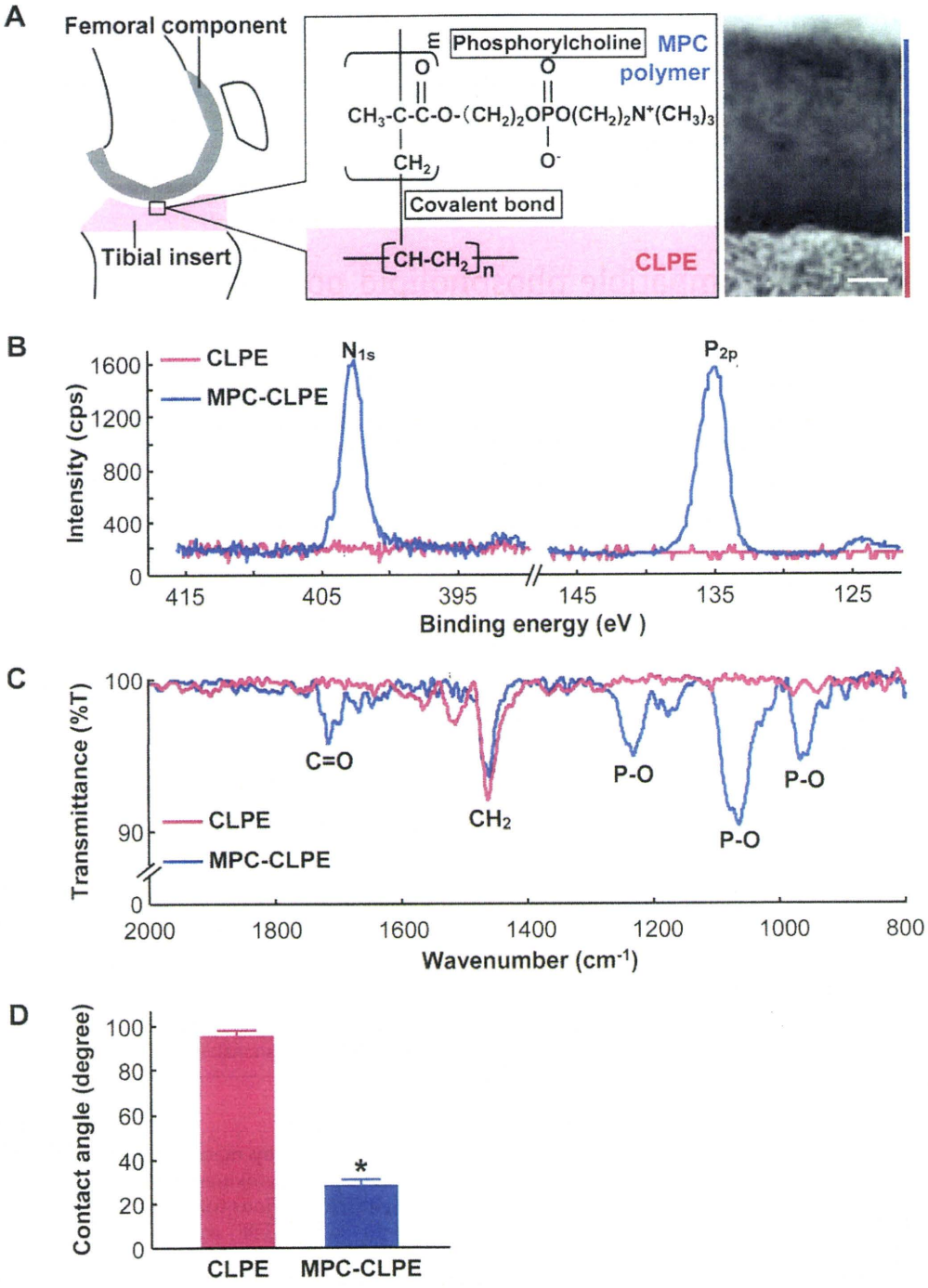

Fig. 1. Analyses of CLPE surfaces with and without MPC grafting. (A) A scheme of the TKA prosthesis with the MPC polymer graft onto the CLPE surface of the tibial insert. The MPC polymer, a biocompatible polymer with side chain composed of phosphorylcholine resembling the phospholipid of biomembrane, is bound to the CLPE insert by the covalent bond with a photoinduced graft polymerization technique. A transmission electron microscope image of the surface is shown on the right. The blue and red lines indicate the MPC layer and the tibial insert surface, respectively (scale bar, 20 nm). (B) X-ray photoelectron spectra of the CLPE and MPC–CLPE surfaces. The peaks in the nitrogen (N_{1s}) and phosphorus (P_{2p}) atom regions at 403 and 135 eV, respectively, are specific to MPC. (C) FT-IR/ATR spectra of the surfaces. Absorptions representing the phosphate group (P–O) at 1240, 1080, and 970 cm^{-1}, and ketone group (C=O) at 1720 cm^{-1} are specific to MPC, while the methylene group (CH_2) at 1460 cm^{-1} is common with and without MPC. (D) Hydrophilicity determined by the contact angle of a water droplet with the CLPE and MPC–CLPE surfaces. Data are expressed as means (bars) ± 95% confidence intervals (CI; error bars) for 10 surfaces/group. *$p < 0.0001$ vs CLPE.

biological reactions and is now clinically used on the surfaces of intravascular stents, soft contact lenses and the artificial lung under the authorization of the Food and Drug Administration (FDA) of the United States[20,21]. Aiming at the elimination of periprosthetic osteolysis in THA, we have developed a novel hip CLPE liner with graft polymerization of MPC on its surface, and found that the grafting dramatically decreased the production of wear particles using the THA simulator[22–25]. The MPC grafting increased the lubricity on the surface of the liner without affecting the physical or mechanical properties of the CLPE substrate[22]. In addition, the MPC-grafted particles were biologically inert and did not cause subsequent bone resorptive responses[24], indicating that this

technology prevents wear particle production and the biologic reaction to such particles in THA. Since we further confirmed the stability of the MPC polymer on the surface even after gamma-ray irradiation for the sterilization[25,26], it is believed that there is probably no theoretical drawback or risk of this technology for clinical use. Besides THA, this technology might possibly be applicable to TKA in which PE particles are also thought to initiate periprosthetic osteolysis[4–6]. A study projected that TKA and THA will grow by 601% and 137%, respectively, between 2005 and 2030[27], indicating that the trend of the increases is considerably more pronounced for TKA than for THA. The increases and future estimates have contributed to our undertaking of the present study on the effects of surface grafting of the MPC polymer on the wear and properties of tibial inserts for the longevity of TKA.

Materials and methods

Materials

Our original TKA system based on STK-01 (Japan Medical Materials Corporation, Osaka, Japan) with posterior cruciate retention design and single radius surface was used for the simulator experiment. For cross-linking, a compression-molded PE (GUR 1020) bar stock was irradiated with a 50 kGy gamma-ray and annealed in nitrogen gas. MPC was synthesized and purified as previously reported[19]. For the grafting, CLPE tibial inserts were placed in the MPC solution (0.5 mol/L), and photoinduced polymerization on the surface was carried out using an ultra-high pressure mercury lamp (UVL-400HA, Riko-Kagaku Sangyo Co., Ltd., Chiba, Japan), as previously reported[23–25,28]. All inserts were sterilized with a 25 kGy gamma-ray in nitrogen gas.

Surface analyses

The elemental conditions of the CLPE surfaces with and without MPC grafting were analyzed using highly sensitive X-ray photoelectron spectroscopy (AXIS-HSi165, Kratos/Shimadzu Corp., Kyoto, Japan). The functional group vibrations of the surfaces were examined by Fourier-transform infrared spectroscopy with attenuated total reflection (FT-IR/ATR; FT/IR615, JASCO Co., Ltd., Tokyo). Hydrophilicity was determined by the static water contact angles on the surfaces of the CLPE and MPC-grafted CLPE (MPC–CLPE) plates using the sessile drop method, according to the International Organization for Standardization (ISO) 15989. Drops of purified water (1 mL) were deposited individually on the plate surface, and the contact angles were directly measured with an optical bench-type contact angle goniometer (Model DM300, Kyowa Interface Science Co., Ltd., Saitama, Japan) after 60 s of dropping.

Friction test

The dynamic coefficients of friction between the PE, CLPE, and MPC–CLPE plates and a cobalt–chromium alloy ball were measured using a ball-on-plate machine (Tribostation 32, Shinto Scientific Co., Ltd., Tokyo), according to the American Society for Testing and Materials (ASTM) F732[29]. The friction tests were performed at room temperature with a load of 0.98 N, sliding distance of 25 mm, and frequency of 1 Hz in distilled water containing 27% bovine serum (Sigma Chemical Corp., MO), 20 mM/L ethylene diamine tetraacetic acid and 0.2 mass% sodium azide.

TKA simulator experiment

A TKA simulator test was performed under the conditions recommended by ISO 14243 using a 6-station TKA apparatus (Advanced Mechanical Technology, Inc., MA) with 6-mm-thick PE, CLPE, or MPC–CLPE tibial inserts against the cobalt–chromium alloy femoral component. The abovementioned distilled water containing 27% bovine serum was used as the lubricant and replaced every 5×10^5 cycles, according to ISO 14243-1. The conditions of stance-phase kinematics were 0°–58° flexion-extension, 5.2 mm anterior–posterior translation, and −1.9°–5.7° internal–external rotation. A simulating physiologic loading curve with a normal gait pattern and 2.60 kN peak load (heel strike = 2.60 kN, toe off = 2.43 kN) was applied at a frequency of 1 Hz, according to ISO 14243-3. The simulator was run up to 5×10^6 cycles for 3 months. At intervals of 5×10^5 cycles the liners were removed from the simulator and weighed on a microbalance (Sartorius GENIUS ME215S, Sartorius AG, Gottingen, Germany) to determine the wear amount. Since the inserts are known to absorb water during their soak in the lubricant[10,30], we also measured the weight gain of the inserts which were axially-loaded cyclically to the femoral components with the same pressure as the TKA simulator, but without rotational motion (load-soak control) according to ISO 14243-2 (section 4.5). The wear amount in the TKA simulator was estimated to be the weight loss of the inserts in the simulator after correction by the average weight gain in the respective load-soak controls.

The morphological change of the inserts was measured using a three-dimensional coordinate measurement instrument (BHN-305, Mitsutoyo Corp., Kawasaki, Japan) and reconstructed using three-dimensional modeling software (Imageware, Siemens PLM Software Inc., TX, USA). To evaluate the actual change of surface morphology caused by wear, the surface of tibial inserts was observed with a confocal scanning laser microscope (OLS1200, Olympus Corp., Tokyo). The remainder of the MPC layer after the simulator test was examined with a transmission electron microscope (JEM-1010, JEOL Ltd., Tokyo) at three spots randomly selected on cross sections of the MPC–CLPE surface. Assessment by the X-ray photoelectron spectrophotometry was difficult due to adhesive proteins that were degraded and precipitated by the friction heat on the surface.

Analyses of wear particles

Wear particles isolated from the lubricant were analyzed according to the ASTM F1877-05 standard. For the isolation, the lubricant after testing was incubated with 5 mol/L NaOH solution for 3 h at 65°C in order to digest adhesive proteins that were degraded and precipitated. To avoid artifacts, contaminating proteins were removed by extraction with sugar solution (1.05 g/cm^3) and isopropyl alcohol solutions (0.98 and 0.90 g/cm^3). After centrifugation at 4,000 rpm for 3 h at 5°C, particles were collected, subjected to sequential filtrations (0.1 μm of minimum pore size)[9,31], and digitally imaged on a scanning electron microscope (S-3400N, Hitachi, Ltd., Tokyo). An image-processing program (Scion image, Scion Corp., Frederick, MD) based on the NIH Image Software was used to measure the total number, area, and volume of wear particles per 10^6 cycles[32,33]. The particle size distribution was expressed by the equivalent circle diameter calculated from the total number and the total area in each insert.

Small punch test

To evaluate the mechanical properties of the tibial inserts before and after the testing, we performed the small punch test, according to ASTM F2183-02[7,34]. Four plugs were harvested from medial and lateral wear-track areas of each insert, perpendicular to the joint surface. Two disk specimens (6.4 mm in diameter and 0.5 mm in thickness) were machined from each plug, representing the surface

and subsurface zones of the insert at depths of 0–0.5 and 1.5–2.0 mm, respectively, from the joint surface. Each disk was placed in a custom-made device consisting of a cylindrical disk holder and a hemispherical-head steel punch, mounted on a compression tester (Instron 5600R1, Instron Corp., Norwood, MA), and deformed by indentation with the punch moving at a displacement rate of 0.5 mm/min.

Statistical analysis

Means of groups were compared by ANOVA and significance of differences was determined by post-hoc testing using Bonferroni's method.

Results

Analyses of CLPE surfaces with and without MPC grafting

The MPC polymer was grafted through photoinduced polymerization onto the CLPE surface of the tibial insert of the TKA prosthesis [Fig. 1(A)]. Successful grafting was confirmed by X-ray photoelectron spectroscopy [Fig. 1(B)] and FT-IR/ATR spectroscopy [Fig. 1(C)]. The spectra for nitrogen and phosphorus atoms were detected only on the MPC–CLPE surface, but not on the CLPE [Fig. 1(B)]. These peaks were characteristic of the phosphorylcholine present in the MPC units, since they were assigned to the $-N^{+}(CH_3)_3$ and phosphate groups, respectively. The FT-IR/ATR spectra representing the phosphate group (P–O) at 1240, 1080 and 970 cm^{-1}, and ketone group (C=O) at 1720 cm^{-1} were also confirmed to be detected only on the plates with MPC grafting [Fig. 1(C)]. The contact angle of a water drop on the MPC–CLPE plate surface was about 1/3 that of the CLPE plate surface [Fig. 1(D)], indicating that MPC grafting increased hydrophilicity.

Effects of cross-linking and MPC grafting on the friction and wear of tibial inserts in a TKA simulator

We initially compared the friction torques of the surfaces of PE, CLPE, and MPC–CLPE plates against a cobalt–chromium alloy femoral ball. Although the cross-linking by itself did not alter the friction torque, the MPC grafting on the CLPE surface decreased it by 88% [Fig. 2(A)].

We then examined the wear of the tibial inserts with or without cross-linking and MPC grafting using a TKA simulator during 5×10^6 cycles of rotational motion and axial-loading against cobalt–chromium alloy femoral components. Considering that the inserts absorb water and gain weight during their soak in the lubricant[10,30], we initially performed a preparatory experiment called load-soak control in which the inserts were axially-loaded cyclically to the femoral components with the same pressure as the TKA simulator, but without rotational motion. The tibial inserts showed comparable weight gains during 5×10^6 cycles, regardless of the presence or absence of cross-linking and MPC grafting [Fig. 2(B)]. We then estimated the wear amount in the TKA simulator as the weight loss of the inserts after correction by the average weight gain in the respective load-soak controls. The corrected weight loss of the non-cross-linked PE insert representing the wear amount was increased in a cycle-dependent manner [Fig. 2(C)]. This was significantly suppressed in the CLPE tibial inserts, clearly demonstrating that the cross-linking provided wear resistance. The MPC–CLPE showed a further decrease in the wear amount. When the corrected weight loss was counted every 10^6 cycle interval, both cross-linking and MPC grafting were shown to maintain similar wear resistance in all intervals (Table I). The MPC–CLPE insert did not lose weight, but instead gained weight even after the correction by water absorption in the load-soak control [Fig. 2(C), Table I], suggesting underestimation of the load-soak control, as pointed out in previous reports[5,7,10,12].

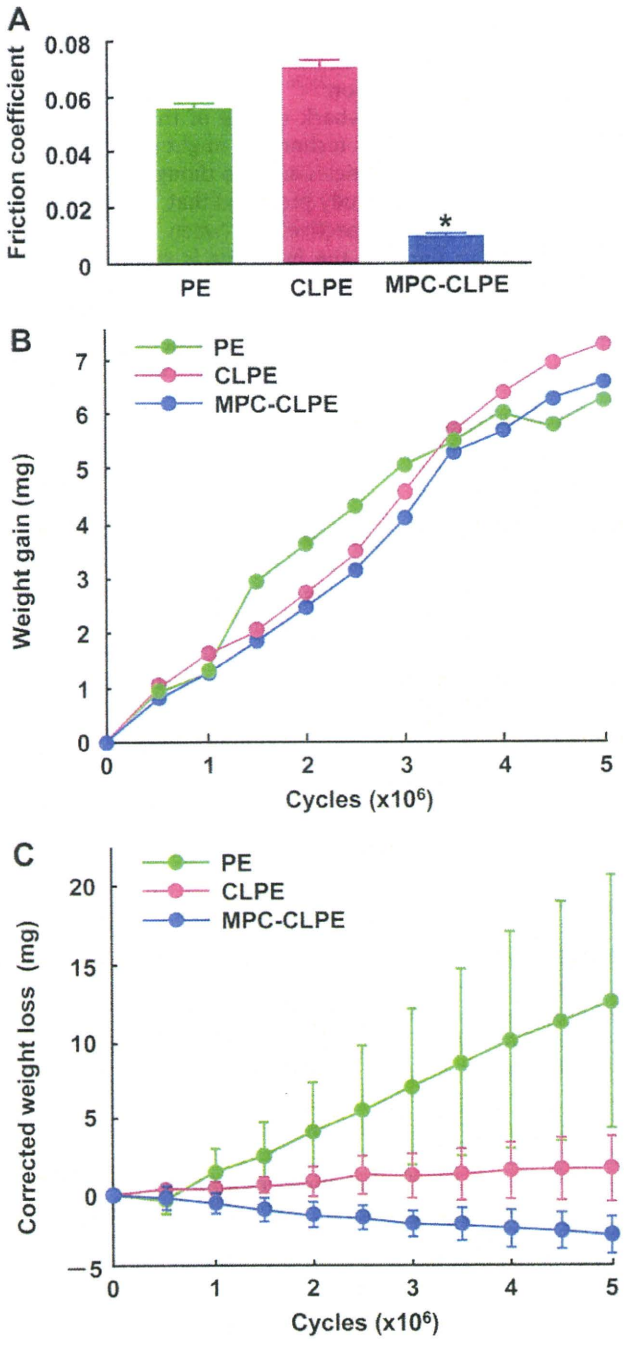

Fig. 2. Friction and wear amounts of tibial inserts with or without cross-linking and MPC grafting in the TKA simulator. (A) Friction torque of surfaces of PE, CLPE, and MPC–CLPE plates against a cobalt–chromium alloy femoral ball. Data are expressed as means (bars) ± 95% confidence intervals (CI; error bars) for three plates/group. *$p < 0.0001$ vs CLPE. (B) Load-soak control experiment. Water absorption of the inserts which were axially-loaded cyclically to the femoral components with the same pressure as the TKA simulator, but without rotational motion. Data are expressed as means (symbols) for two inserts/group. (C) Time course of wear amount in the TKA simulator during 5×10^6 cycles of rotational motion and axial-loading against cobalt–chromium alloy femoral components. The amount was estimated from the weight loss of the inserts after correction by the average weight gain in the respective load-soak controls as shown in (B) (weight loss in the TKA simulator + average of weight gain in the load-soak control). Data are expressed as means (symbols) ± 95% CI (error bars) for three inserts/group. *p*-values in every 10^6 cycle interval are shown in Table I.

Table I
Wear amount estimated by the corrected weight loss in every 10^6 cycle interval

Cycles ($\times 10^6$)	PE	CLPE		MPC–CLPE	
			P-value (vs PE)		P-value (vs CLPE)
0–1	1.47 (−1.79–3.01)	0.37 (−0.08–0.81)	0.0895	−0.60 (−1.28–0.08)	0.0098
1–2	2.65 (0.89–4.40)	0.31 (−0.19–0.82)	0.0061	−0.85 (−1.06–−0.63)	<0.0001
2–3	2.98 (1.11–4.85)	0.52 (0.03–1.00)	0.0063	−0.55 (−0.59–−0.51)	<0.0001
3–4	3.04 (1.03–5.05)	0.36 (−0.08–0.81)	0.0053	−0.26 (−0.66–0.13)	0.0193
4–5	2.50 (1.12–3.88)	0.09 (−0.15–0.34)	0.0004	−0.40 (−0.48–−0.33)	0.0001
Average	2.53 (0.90–4.15)	0.33 (0.26–0.40)	0.0051	−0.53 (−0.77–−0.30)	<0.0001

Data except the *p*-values are expressed as means and 95% CI in parentheses of mg/10^6 cycles for three inserts/group.

Time course of three-dimensional morphometric analyses of medial and lateral surfaces of the three kinds of tibial inserts confirmed the wear resistance by the cross-linking and MPC grafting [Fig. 3(A)]. During testing up to 5×10^6 cycles, the cross-linking increased the wear resistance as compared to the non-cross-linked PE, and the MPC grafting further enhanced it. Confocal scanning laser microscopic analyses of the insert surfaces revealed that the original machine marks that were clearly visible before the testing still remained on the MPC–CLPE surfaces even after 5×10^6 cycles, while they were completely obliterated not only on the non-cross-linked PE, but also on the CLPE surfaces [Fig. 3(B)]. Furthermore, the transmission electron microscope analysis showed that two out of three randomly selected spots on an MPC–CLPE surface were covered by the MPC polymer layer even after 5×10^6 cycles of testing [Fig. 3(C)].

When we analyzed the wear particles isolated from lubricants in the TKA simulator, the amounts shown by the total number, area, and volume of particles were decreased by cross-linking, and were almost abrogated by the MPC grafting [Fig. 4(A)]. However, there was no significant difference of the particle size distribution among the three inserts, the great majority of them being 0.5–1.0 μm [Fig. 4(B)], as previously reported[35,36].

Effects of cross-linking and MPC grafting on mechanical properties of tibial inserts in a TKA simulator

In addition to the wear resistance, the mechanical properties of the tibial insert are another important factor in the longevity, since contact stress during activities of daily living are thought to be stronger in the knee joint than in the hip joint, due to low conformity and the small contact area in the tibiofemoral joint geometry[5,9]. Hence, we compared the mechanical properties of the three kinds of inserts before and after 5×10^6 cycles by the small punch test on the surface and subsurface specimens (Table II). As previously reported[7,34], cross-linking slightly, although not significantly, reduced the ultimate displacement and the work to failure, but not the ultimate load, before the testing, indicating a decrease in elasticity. However, the MPC grafting altered neither of the parameters of the CLPE inserts, nor was there any difference between before and after the testing in the three kinds of inserts. Furthermore, there was no difference between the surface and subsurface specimens even after the testing. These findings indicate that the mechanical properties remain unchanged during the testing, regardless of the presence or absence of cross-linking and MPC grafting.

Discussion

Although a series of our previous studies have shown that MPC grafting is promising to extend the longevity of THA[22–25,28], this might not be true for TKA due to different mechanisms of motion between hip and knee joints. Unlike the highly congruent ball-and-socket articulation in the hip joint, the geometry and articulation of the knee joint is complex. Hence, in TKA, PE wear occurs from a combination of rolling, sliding, and rotational motions over the bearing surface, so that this may lead to delamination, pitting, and fatigue failure of the PE surface. Contrarily, the wear in THA occurs primarily as a result of microadhesion and microabrasion[5]. Despite the mechanistic difference, the present study revealed that the MPC grafting is also promising for the TKA longevity, similarly to THA.

The MPC grafting increased hydrophilicity and decreased the friction [Figs. 1(D) & 2(A)], and our previous study showed that the water fraction on the MPC polymer surface is kept at a higher level[37]. Although the MPC polymer layer partially remained even after the TKA simulator experiment [Fig. 3(C)], the load-soak control experiment showed that the weight gain was similarly seen regardless of the presence or absence of the MPC grafting [Fig. 2 (B)]. These confirm that the reduction of the insert weight loss by MPC grafting is not due to the weight of water itself retained in the remaining MPC layer, but due to the wear resistance caused by the water fraction. Hence, as in natural synovial joints[16,17], the enhancement of wear resistance is likely attributable to the fluid film lubrication by the intermediate hydrated layer formed by the MPC polymer that contains phosphorylcholine mimicking the natural phospholipids[19].

Although the difference in the effectiveness of cross-linking between THA and TKA is controversial, several studies using TKA simulators have reported the preventive effect on the insert wear[7–13]. Among the reports, Fisher *et al.* reported the wear rates per 10^6 cycles being 13.8 ± 4.3 mg in CLPE vs 24.5 ± 6.4 mg in the conventional PE[9]. Muratoglu *et al.* reported 0.7 ± 0.1 mg in aged CLPE, 8.8 ± 1.5 mg in conventional PE, and 9.6 ± 3.6 mg in aged conventional PE[10]; and recently 5.3 ± 2.1 mg in CLPE vs 16.0 ± 4.3 mg in conventional PE[11]. The present wear rates were 0.3 ± 0.4 mg in CLPE vs 2.5 ± 1.6 mg in conventional PE (Table I). Although the absolute values are different among the reports, probably dependent on several factors like protocol of the simulator test, design of the implant, degree of cross-linking and method of sterilization, all reports support the preventive effects on the PE wear, similarly to THA. Unlike the MPC grafting, cross-linking suppressed the wear production without affecting the friction [Fig. 2(A)]. This implies that cross-linking does not alter the surface lubricity, but was responsible for the resistance to wear, probably by improving the mechanical properties. However, it has been shown that mechanical properties of a PE insert decrease depending on the irradiation dosage, causing fatigue and brittleness[38,39]. A recent report using a small punch test after the TKA simulator experiment showed that a simulator-tested PE that had received more than 150 kGy showed lower toughness, but one that had received 35–75 kGy exhibited somewhat higher toughness than equivalent material without irradiation, suggesting that an optimal irradiation dose for cross-linking would be less than 100 kGy[7]. In the present study, we selected 50 kGy irradiation for the cross-linking, and in fact, none of the parameters of the small

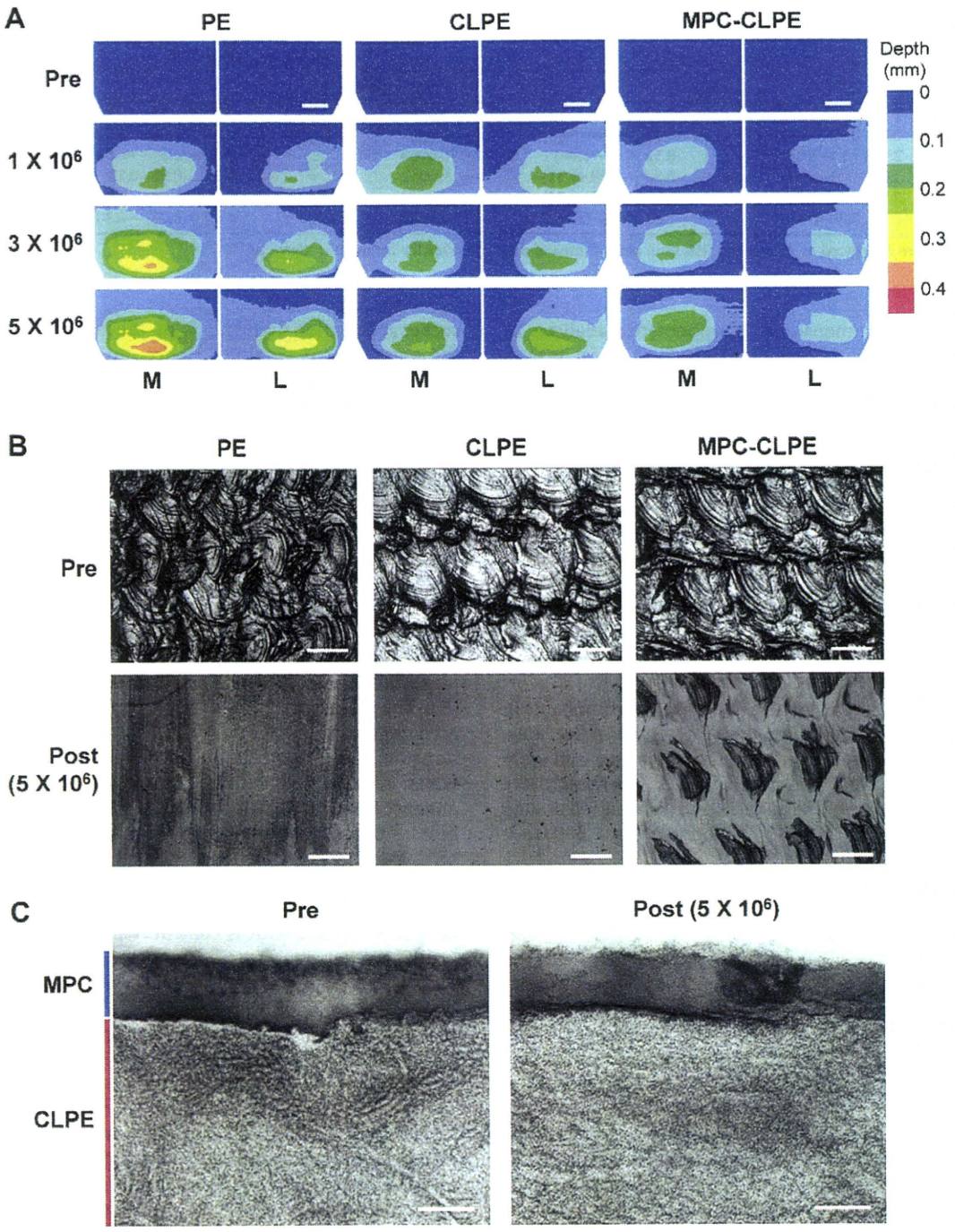

Fig. 3. Optical findings of the surfaces of the three inserts in the TKA simulator. (A) Three-dimensional morphometric analyses of medial (M) and lateral (L) surfaces of the PE, CLPE, and MPC–CLPE inserts before (pre) and after 1, 3, 5×10^6 cycles. Scale bars, 5 mm. (B) Confocal scanning laser microscopic analysis of the medial contact areas in the three insert surfaces before (pre) and after 5×10^6 cycles (post). Scale bars, 100 μm. (C) Transmission electron microscope images of one of three randomly selected spots on the surface of an MPC–CLPE insert before (pre) and after 5×10^6 cycles (post). Scale bars, 100 nm.

punch test changed after the simulator testing, although the parameters of elasticity (ultimate displacement and the work to failure) were slightly decreased before the testing.

In addition to enhancement of wear resistance of the tibial inserts, reduction of bone resorptive responses to wear particles generated is important for the prevention of periprosthetic osteolysis. The responses are dependent not only on the total amount of particles, but also on the proportion of those which are within the most biologically active size range[40]. The present analysis of the wear particles isolated from lubricants in the TKA simulator revealed that cross-linking and MPC grafting dramatically decreased the total amount of particles with little effect on the particle size (Fig. 4). Since the majority from the three kinds of inserts were submicrometer and nanometer-sized particles which are consistent with previous reports[35,36] and known to induce inflammatory responses[40–42], the suppression of particle amount by the cross-linking and MPC grafting will aid in the effective prevention of periprosthetic osteolysis.

One limitation of this study is the confined period of simulator testing. Although the 5×10^6 cycles in the TKA simulator

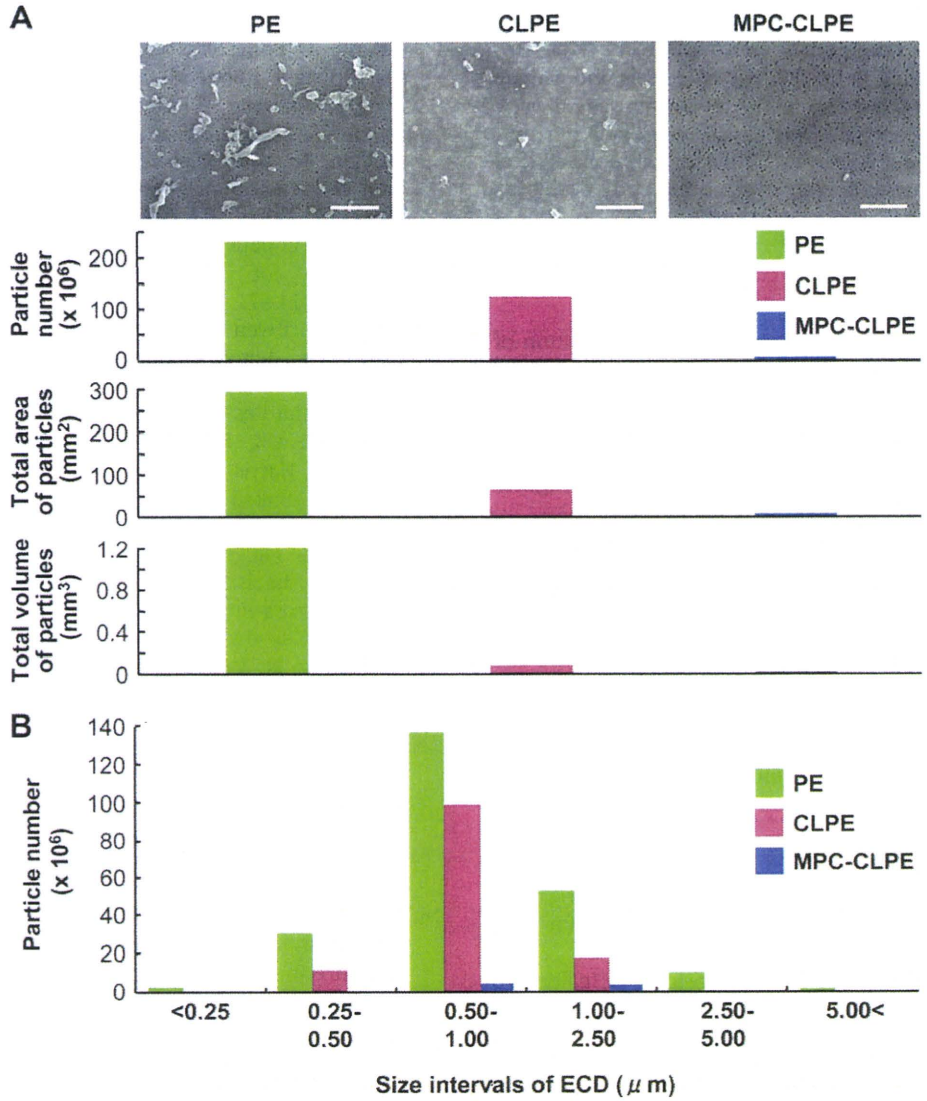

Fig. 4. Analyses of wear particles isolated from lubricants in the TKA simulator. (A) Scanning electron microscopic images of the wear particles from PE, CLPE, and MPC–CLPE inserts. Scale bars, 5 μm. The graphs below show the total number, area, and volume of wear particles per 10^6 cycles. (B) Number of particles per 10^6 cycles in each size range of equivalent circle diameter from PE, CLPE, and MPC–CLPE inserts.

are comparable to 5–10 years of physical walking, this may not be long enough for young active patients with rheumatoid arthritis or fracture. We are now running the TKA simulator longer, and so far have confirmed almost no wear on the MPC–CLPE tibial inserts after 1×10^7 cycles. Another limitation of the TKA simulator experiment is that it does not entirely capture the range of loading conditions of a knee, in terms of either the variety of positions or the magnitude of loading, although we nonetheless believe this experiment can provide some indication of trends.

Table II
Small punch test to measure the mechanical properties of the PE, CLPE, and MPC–CLPE inserts before (pre) and after 5×10^6 cycles (post)

		PE		CLPE		MPC–CLPE	
		Pre	Post	Pre	Post	Pre	Post
Ultimate displacement (mm)	Surface	4.3 (4.1–4.5)	4.4 (4.3–4.5)	3.4 (3.2–3.6)	3.4 (3.3–3.5)	3.5 (3.2–3.8)	3.6 (3.5–3.7)
	Subsurface	4.2 (4.1–4.3)	4.3 (4.3–4.4)	3.6 (3.5–3.7)	3.6 (3.5–3.7)	3.7 (3.5–3.9)	3.7 (3.6–3.8)
Ultimate load (*N*)	Surface	63.1 (62.5–63.7)	61.3 (60.9–61.7)	61.9 (58.5–65.3)	62.5 (62.1–62.9)	65.8 (56.8–74.8)	60.5 (54.8–66.2)
	Subsurface	63.7 (63.1–64.3)	62.5 (61.2–63.8)	62.2 (61.9–62.6)	62.3 (61.5–63.1)	64.9 (60.8–69.0)	62.9 (60.7–65.1)
Work to failure (mJ)	Surface	196.6 (186.0–207.2)	202.9 (197.3–208.6)	149.0 (129.9–168.1)	147.6 (142.0–153.2)	156.3 (123.4–189.2)	157.0 (147.2–166.8)
	Subsurface	201.6 (197.6–205.6)	211.3 (200.7–221.9)	166.9 (155.9–177.9)	176.8 (170.7–182.9)	177.2 (161.0–193.4)	181.5 (177.4–185.7)

Ultimate displacement, ultimate load, and work to failure of disk specimens (6.4 mm in diameter and 0.5 mm in thickness) taken from the surface (0–0.5 mm in depth) and subsurface (1.5–2.0 mm in depth) of the inserts. Data are expressed as means and 95 % CI in parentheses for 8 disks/group. There was no significant difference among the three groups ($p > 0.05$).

From the present simulator experiment, we speculate that the MPC grafting may make a significant improvement in total joint replacements by preventing periprosthetic osteolysis and aseptic loosening not only in THA, but also in TKA. However, several variations of PE have been reported in the past to work well in simulators, but were not successful *in vivo*[43,44]. In addition to the clinical trial of THA which is now underway, we are currently designing a trial for TKA to evaluate its clinical efficiency.

Author contributions

(1) The conception and design of the study, or acquisition of data, or analysis and interpretation of data.

Toru Moro (moro-ort@h.u-tokyo.ac.jp), Yoshio Takatori (takatori-ort@h.u-tokyo.ac.jp), Masayuki Kyomoto (kyomotom@jmmc.jp), Ken-ichi Saiga (saigak@jmmc.jp), Kozo Nakamura (nakamurak-ort@h.u-tokyo.ac.jp), and Hiroshi Kawaguchi (kawaguchi-ort@h.u-tokyo.ac.jp).

(2) Drafting the article or revising it critically for important intellectual content.

Toru Moro, Kazuhiko Ishihara (ishihara@mpc.t.u-tokyo.ac.jp), and Hiroshi Kawaguchi.

(3) Final approval of the version to be submitted.

All authors.

Conflicts of interest

The authors declare that there is no conflict of interest.

Acknowledgments

We thank Noboru Yamawaki, Masaru Ueno, Akinori Mori, Kazuhiro Yoshida, Tomohiro Konno and Reiko Yamaguchi for their excellent technical assistance.

Source of funding: This study was supported by Health and Welfare Research Grant for Translational Research (H17-005), Research on Medical Devices for Improving Impaired QOL (H20-004) from the Japanese Ministry of Health, Labor and Welfare. The sponsor had no role in study design, data collection, data analysis, data interpretation, or writing of the manuscript.

Supplementary data

Supplementary data associated with this article can be found in the online version at doi:10.1016/j.joca.2010.05.019.

References

1. Kim S. Changes in surgical loads and economic burden of hip and knee replacements in the US: 1997–2004. Arthritis Rheum 2008;59:481–8.
2. Kurtz SM, Mowat F, Ong K, Chan N, Lau E, Halpern M. Prevalence of primary and revision total hip and knee arthroplasty in the United States from 1990 through 2002. J Bone Joint Surg Am 2005;87:1487–97.
3. Sharkey PF, Hozack WJ, Rothman RH, Shastri S, Jacoby SM. Insall Award paper. Why are total knee arthroplasties failing today? Clin Orthop Relat Res 2002;404:7–13.
4. Jacobs JJ, Roebuck KA, Archibeck M, Hallab NJ, Glant TT. Osteolysis: basic science. Clin Orthop Relat Res 2001;393:71–7.
5. Naudie DD, Ammeen DJ, Engh GA, Rorabeck CH. Wear and osteolysis around total knee arthroplasty. J Am Acad Orthop Surg 2007;15:53–64.
6. Glant TT, Jacobs JJ, Molnar G, Shanbhag AS, Valyon M, Galante JO. Bone resorption activity of particulate-stimulated macrophages. J Bone Miner Res 1993;8:1071–9.
7. Akagi M, Asano T, Clarke IC, Niiyama N, Kyomoto M, Nakamura T, *et al.* Wear and toughness of crosslinked polyethylene for total knee replacements: a study using a simulator and small-punch testing. J Orthop Res 2006;24:2021–7.
8. Chiesa R, Tanzi MC, Alfonsi S, Paracchini L, Moscatelli M, Cigada A. Enhanced wear performance of highly crosslinked UHMWPE for artificial joints. J Biomed Mater Res 2000;50:381–7.
9. Fisher J, McEwen HM, Tipper JL, Galvin AL, Ingram J, Kamali A, *et al.* Wear, debris, and biologic activity of cross-linked polyethylene in the knee: benefits and potential concerns. Clin Orthop Relat Res 2004;428:114–9.
10. Muratoglu OK, Bragdon CR, Jasty M, O'Connor DO, Von Knoch RS, Harris WH. Knee-simulator testing of conventional and cross-linked polyethylene tibial inserts. J Arthroplasty 2004;19:887–97.
11. Muratoglu OK, Rubash HE, Bragdon CR, Burroughs BR, Huang A, Harris WH. Simulated normal gait wear testing of a highly cross-linked polyethylene tibial insert. J Arthroplasty 2007;22:435–44.
12. Tsukamoto R, Williams PA, Clarke IC, Pezzotti G, Shoji H, Akagi M, *et al.* Y-TZP zirconia run against highly crosslinked UHMWPE tibial inserts: knee simulator wear and phase-transformation studies. J Biomed Mater Res B Appl Biomater 2008;86:145–53.
13. Tsukamoto R, Williams PA, Shoji H, Hirakawa K, Yamamoto K, Tsukamoto M, *et al.* Wear in molded tibial inserts: knee simulator study of H1900 and GUR1050 polyethylenes. J Biomed Mater Res B Appl Biomater 2008;85:314–9.
14. D'Antonio JA, Manley MT, Capello WN, Bierbaum BE, Ramakrishnan R, Naughton M, *et al.* Five-year experience with Crossfire highly cross-linked polyethylene. Clin Orthop Relat Res 2005;441:143–50.
15. Dorr LD, Wan Z, Shahrdar C, Sirianni L, Boutary M, Yun A. Clinical performance of a Durasul highly cross-linked polyethylene acetabular liner for total hip arthroplasty at five years. J Bone Joint Surg Am 2005;87:1816–21.
16. Dowson D, Jin ZM. Micro-elastohydrodynamic lubrication of synovial joints. Eng Med 1986;15:63–5.
17. Hills BA. Boundary lubrication in vivo. Proc Inst Mech Eng [H] 2000;214:83–94.
18. Kirk TB, Wilson AS, Stachowiak GW. The morphology and composition of the superficial zone of mammalian articular cartilage. J Orthop Rheumatol 1993;6:21–8.
19. Ishihara K, Ueda T, Nakabayashi N. Preparation of phospholipid polymers and their properties as polymer hydrogel membrane. Polym J 1990;22:355–60.
20. Ishihara K, Shinozuka T, Hanazaki Y, Iwasaki Y, Nakabayashi N. Improvement of blood compatibility on cellulose hemodialysis membrane: IV. Phospholipid polymer bonded to the membrane surface. J Biomater Sci Polym Ed 1999;10:271–82.
21. Yoneyama T, Sugihara K, Ishihara K, Iwasaki Y, Nakabayashi N. The vascular prosthesis without pseudointima prepared by antithrombogenic phospholipid polymer. Biomaterials 2002;23:1455–9.
22. Kyomoto M, Moro T, Konno T, Takadama H, Kawaguchi H, Takatori Y, *et al.* Effects of photo-induced graft polymerization of 2-methacryloyloxyethyl phosphorylcholine on physical properties of cross-linked polyethylene in artificial hip joints. J Mater Sci Mater Med 2007;18:1809–15.
23. Kyomoto M, Moro T, Konno T, Takadama H, Yamawaki N, Kawaguchi H, *et al.* Enhanced wear resistance of modified

cross-linked polyethylene by grafting with poly(2-methacryloyloxyethyl phosphorylcholine). J Biomed Mater Res A 2007;82:10–7.
24. Moro T, Takatori Y, Ishihara K, Konno T, Takigawa Y, Matsushita T, *et al.* Surface grafting of artificial joints with a biocompatible polymer for preventing periprosthetic osteolysis. Nat Mater 2004;3:829–36.
25. Moro T, Takatori Y, Ishihara K, Nakamura K, Kawaguchi H. 2006 Frank Stinchfield Award: grafting of biocompatible polymer for longevity of artificial hip joints. Clin Orthop Relat Res 2006;453:58–63.
26. Kyomoto M, Moro T, Miyaji F, Konno T, Hashimoto M, Kawaguchi H, *et al.* Enhanced wear resistance of orthopaedic bearing due to the cross-linking of poly(MPC) graft chains induced by gamma-ray irradiation. J Biomed Mater Res B Appl Biomater 2008;84:320–7.
27. Kurtz SM, Ong K, Lau E, Mowat F, Halpern M. Projections of primary and revision hip and knee arthroplasty in the United States from 2005 to 2030. J Bone Joint Surg Am 2007;89:780–5.
28. Moro T, Kawaguchi H, Ishihara K, Kyomoto M, Karita T, Ito H, *et al.* Wear resistance of artificial hip joints with poly (2-methacryloyloxyethyl phosphorylcholine) grafted polyethylene: comparisons with the effect of polyethylene cross-linking and ceramic femoral heads. Biomaterials 2009;30:2995–3001.
29. Kumar P, Oka M, Ikeuchi K, Shimizu K, Yamamuro T, Okumura H, *et al.* Low wear rate of UHMWPE against zirconia ceramic (Y-PSZ) in comparison to alumina ceramic and SUS 316L alloy. J Biomed Mater Res 1991;25:813–28.
30. Schwenke T, Kaddick C, Schneider E, Wimmer MA. Fluid composition impacts standardized testing protocols in ultra-high molecular weight polyethylene knee wear testing. Proc Inst Mech Eng H 2005;219:457–64.
31. Tipper JL, Ingham E, Hailey JL, Besong AA, Fisher J, Wroblewski BM, *et al.* Quantitative analysis of polyethylene wear debris, wear rate and head damage in retrieved Charnley hip prostheses. J Mater Sci Mater Med 2000;11:117–24.
32. Campbell P, Doorn P, Dorey F, Amstutz HC. Wear and morphology of ultra-high molecular weight polyethylene wear particles from total hip replacements. Proc Inst Mech Eng H 1996;210:167–74.
33. Dean DD, Schwartz Z, Liu Y, Blanchard CR, Agrawal CM, Mabrey JD, *et al.* The effect of ultra-high molecular weight polyethylene wear debris on MG63 osteosarcoma cells in vitro. J Bone Joint Surg Am 1999;81:452–61.
34. Kurtz SM, Foulds JR, Jewett CW, Srivastav S, Edidin AA. Validation of a small punch testing technique to characterize the mechanical behaviour of ultra-high-molecular-weight polyethylene. Biomaterials 1997;18:1659–63.
35. Beaule PE, Campbell PA, Walker PS, Schmalzried TP, Dorey FJ, Blunn GW, *et al.* Polyethylene wear characteristics in vivo and in a knee stimulator. J Biomed Mater Res 2002;60:411–9.
36. Tipper JL, Galvin AL, Williams S, McEwen HM, Stone MH, Ingham E, *et al.* Isolation and characterization of UHMWPE wear particles down to ten nanometers in size from in vitro hip and knee joint simulators. J Biomed Mater Res A 2006;78:473–80.
37. Ishihara K, Nomura H, Mihara T, Kurita K, Iwasaki Y, Nakabayashi N. Why do phospholipid polymers reduce protein adsorption? J Biomed Mater Res 1998;39:323–30.
38. Edidin AA, Pruitt L, Jewett CW, Crane DJ, Roberts D, Kurtz SM. Plasticity-induced damage layer is a precursor to wear in radiation-cross-linked UHMWPE acetabular components for total hip replacement. Ultra-high-molecular-weight polyethylene. J Arthroplasty 1999;14:616–27.
39. Kurtz SM, Pruitt LA, Jewett CW, Foulds JR, Edidin AA. Radiation and chemical crosslinking promote strain hardening behavior and molecular alignment in ultra high molecular weight polyethylene during multi-axial loading conditions. Biomaterials 1999;20:1449–62.
40. Green TR, Fisher J, Stone M, Wroblewski BM, Ingham E. Polyethylene particles of a 'critical size' are necessary for the induction of cytokines by macrophages in vitro. Biomaterials 1998;19:2297–302.
41. Galvin AL, Tipper JL, Ingham E, Fisher J. Nanometre size wear debris generated from crosslinked and non-crosslinked ultra high molecular weight polyethylene in artificial joints. Wear 2005;259:977–83.
42. Ingram JH, Stone M, Fisher J, Ingham E. The influence of molecular weight, crosslinking and counterface roughness on TNF-alpha production by macrophages in response to ultra high molecular weight polyethylene particles. Biomaterials 2004;25:3511–22.
43. Ahn NU, Nallamshetty L, Ahn UM, Buchowski JM, Rose PS, Lemma MA, *et al.* Early failure associated with the use of Hylamer-M spacers in three primary AMK total knee arthroplasties. J Arthroplasty 2001;16:136–9.
44. Wright TM, Rimnac CM, Faris PM, Bansal M. Analysis of surface damage in retrieved carbon fiber-reinforced and plain polyethylene tibial components from posterior stabilized total knee replacements. J Bone Joint Surg Am 1988;70:1312–9.

Colloids and Surfaces B: Biointerfaces 79 (2010) 357–364

Contents lists available at ScienceDirect

Colloids and Surfaces B: Biointerfaces

journal homepage: www.elsevier.com/locate/colsurfb

Simple surface modification of a titanium alloy with silanated zwitterionic phosphorylcholine or sulfobetaine modifiers to reduce thrombogenicity

Sang-Ho Ye[a,b], Carl A. Johnson Jr.[a,c], Joshua R. Woolley[a,c], Hironobu Murata[a,c], Lara J. Gamble[e], Kazuhiko Ishihara[f], William R. Wagner[a,b,c,d,*]

[a] McGowan Institute for Regenerative Medicine, University of Pittsburgh, Pittsburgh, PA 15219, USA
[b] Department of Surgery, University of Pittsburgh, Pittsburgh, PA 15219, USA
[c] Department of Bioengineering, University of Pittsburgh, Pittsburgh, PA 15219, USA
[d] Department of Chemical Engineering, University of Pittsburgh, Pittsburgh, PA 15219, USA
[e] Department of Bioengineering and NESAC/BIO, University of Washington, Seattle, WA 98195, USA
[f] Department of Materials Engineering, School of Engineering, The University of Tokyo, 7-3-1, Hongo, Bunkyo-ku, Tokyo 113-8656, Japan

ARTICLE INFO

Article history:
Received 16 March 2010
Received in revised form 16 April 2010
Accepted 19 April 2010
Available online 24 April 2010

Keywords:
Surface modification
Phosphorylcholine
Sulfobetaine
Blood compatibility
Cardiovascular devices

ABSTRACT

Thrombosis and thromboembolism remain problematic for a large number of blood contacting medical devices and limit broader application of some technologies due to this surface bioincompatibility. In this study we focused on the covalent attachment of zwitterionic phosphorylcholine (PC) or sulfobetaine (SB) moieties onto a $TiAl_6V_4$ surface with a single step modification method to obtain a stable blood compatible interface. Silanated PC or SB modifiers (PCSi or SBSi) which contain an alkoxy silane group and either PC or SB groups were prepared respectively from trimethoxysilane and 2-methacryloyloxyethyl phosphorylcholine (MPC) or *N*-(3-sulfopropyl)-*N*-(methacryloxyethyl)-*N*,*N*-dimethylammonium betaine (SMDAB) monomers by a hydrosilylation reaction. A cleaned and oxidized $TiAl_6V_4$ surface was then modified with the PCSi or SBSi modifiers by a simple surface silanization reaction. The surface was assessed with X-ray photoelectron spectroscopy (XPS), attenuated total reflection-Fourier transform infrared spectroscopy (ATR-FTIR) and contact angle goniometry. Platelet deposition and bulk phase activation were evaluated following contact with anticoagulated ovine blood. XPS results verified successful modification of the PCSi or SBSi modifiers onto $TiAl_6V_4$ based on increases in surface phosphorous or sulfur respectively. Surface contact angles in water decreased with the addition of hydrophilic PC or SB moieties. Both the PCSi and SBSi modified $TiAl_6V_4$ surfaces showed decreased platelet deposition and bulk phase platelet activation compared to unmodified $TiAl_6V_4$ and control surfaces. This single step modification with PCSi or SBSi modifiers offers promise for improving the surface hemocompatibility of $TiAl_6V_4$ and is attractive for its ease of application to geometrically complex metallic blood contacting devices.

1. Introduction

Platelet deposition still occurs on the metallic surfaces utilized in cardiovascular applications such as vascular stents, heart valves, and ventricular assist devices (VADs). As a result, patients implanted with these devices often require chronic anticoagulation or anti-platelet therapy to reduce the risks of thrombosis and thromboembolism. Unfortunately, this pharmacologic therapy comes with an increased risk of bleeding which can result in significant morbidity and mortality [1–5]. Enhancing the thromboresistance of metallic blood contacting surfaces could thus lead to more widespread application of cardiovascular devices with lower complication risks and potentially permit the development of new areas for device application.

To enhance the thromboresistance of VADs in particular, several types of coatings such as titanium nitride (TiN), diamond-like carbon (DLC), 2-methacryloyloxyethyl phosphorylcholine (MPC) polymer, and heparin coatings have been applied to metallic blood contacting surfaces [5]. MPC-based coatings, are notable in that the biomimetic and zwitterionic phosphorylcholine (PC) group-bearing polymers have demonstrated attractive levels of blood compatibility by inhibition of protein adsorption, platelet adhesion and platelet activation on modified surfaces [6–11] and they have been applied onto a variety of metallic surfaces such as vascular stents and VADs [12–15].

In a previous study assessing the preclinical biocompatibility of VAD coatings [15], a physically adsorbed MPC copolymer coating showed superior performance to a DLC coating, a more common

* Corresponding author at: McGowan Institute for Regenerative Medicine, 450 Technology Dr., Suite 300, Pittsburgh, PA 15219, USA. Tel.: +1 412 624 5324; fax: +1 412 624 5363.
E-mail address: wagnerwr@upmc.edu (W.R. Wagner).

0927-7765/$ – see front matter © 2010 Elsevier B.V. All rights reserved.
doi:10.1016/j.colsurfb.2010.04.018

coating for VADs. While DLC coatings have also demonstrated good hemocompatibility and durability independently of comparative studies with MPC, they also carry the risk of microcrack formation [16]. Unlike heparin coated surfaces, MPC copolymer coatings have not been shown to present a potential risk for heparin-induced thrombocytopenia and should be less susceptible to degradative enzymatic process that can act on heparin [17–19]. However physically adsorbed PC group-bearing polymer coatings are not as stable as DLC coatings and the concern of surface stability in long-term applications may offset its perceived advantages. MPC coatings that are covalently linked onto metallic surfaces would thus be more attractive to ensure sustained non-thrombotic properties in long-term cardiovascular applications [13,16].

Along these lines, we have recently demonstrated that a PC group-bearing polymer could be covalently bound to a titanium alloy ($TiAl_6V_4$) surface by a condensation reaction or with plasma initiated graft polymerization after the $TiAl_6V_4$ surface was treated with a functional silane coupling agent [20,21]. However, the required pre-modification steps for these reactions may have resulted in diminished control of the uniformity and coverage of the PC groups on the modified surface. A simplified surface modification technique would be attractive as it could potentially result in better control of the coating process and increase the ease and reproducibility of the coating process for bulk manufacturing as well as reduce the amount of MPC necessary for coating and thereby reduce the overall cost of the coating process.

The aim of our study was to develop a surface modification strategy to obtain a stable blood compatible interface on a $TiAl_6V_4$ surface. This surface has relevance for a number of cardiovascular devices, particularly in the rotary blood pump field where there is interest in extending this type of device therapy to the pediatric population [22]. In the present study, we focused on developing a simple modification method to covalently attach hemocompatible moieties onto a $TiAl_6V_4$ surface in a process that would be amenable to complex surfaces such as one would encounter in a rotary blood pump. For this, we prepared a silanated PC modifier (PCSi) which contains an alkoxy silane and PC groups to modify a clinically relevant $TiAl_6V_4$ surface in a single step. Additionally, in an effort with similar objectives, a silanated sulfobetaine (SB) modifier (SBSi) was also prepared. Surfaces modified with SB group-bearing polymers with zwitterionic side groups [$-N^+(CH_2)_nSO_3^-$] have also exhibited anti-bioadherent properties and non-thrombogenicity due to the ability of the surface to resist protein adsorption and platelet adhesion similar to PC group modified surfaces [23–27]. The modification effect of PCSi and SBSi modifiers on a $TiAl_6V_4$ surface was characterized and the blood compatibility of the modified surfaces was assessed in terms of platelet adhesion and activation following acute blood contact in vitro.

2. Materials and methods

2.1. Materials

Titanium alloy ($TiAl_6V_4$) was purchased (California Metal & Supply Inc., Gardena, CA) and polished with 3.0, 1.0, 0.25, and 0.1 μm diamond pastes (Electron Microscopy Sciences, Washington, PA). The polishing methodology utilized with increasingly fine pastes was matched to that employed for rotary blood pumps under development by Launchpoint Technologies (Goleta, CA). The MPC was obtained from NOF Corporation (Tokyo, Japan), and synthesized by the same method described in a previous report [6]. *N*-(3-sulfopropyl)-*N*-(methacryloxyethyl)-*N*,*N*-dimethylammonium betaine (SMDAB), trimethoxy silane (TMSi) and platinum 10 wt% on activated carbon (Pt/C) were purchased from Sigma–Aldrich (St. Louis, MO).

2.2. Synthesis of silanated zwitterionic modifier

Silanated zwitterionic surface modifiers (PCSi or SBSi) were prepared from TMSi and either MPC or SMDAB monomers by a hydrosilylation reaction. A round bottom flask equipped with magnetic stirrer was charged with anhydrous MeOH (10 mL), and MPC or SMDAB monomer (1 mmol) was dissolved under Ar gas for 30 min. TMSi (10 mmol) was then added in excess and Pt/C (0.1 g) was added as a catalyst followed by flushing with Ar gas for 10 min and sealing of the flask. The mixture was reacted at 40 °C for 24 h in an oil bath. Unreacted TMSi monomer and solvent were removed by a rotary evaporator at 40 °C under reduced pressure. After evaporation, anhydrous MeOH was added and the product filtered with a 25 mm syringe filter (poly(tetrafluoroethylene) (PTFE), 0.45 μm, Corning Inc., Corning, NY) to remove the Pt/C. MeOH was removed again by rotary evaporation. The brown, oil-like reaction product was stored in refrigerator at 4 °C after sealing the container to exclude moisture (Fig. 1). The chemical structures of the silanated PC and SB (PCSi and SBSi) were confirmed with ^1H NMR (300 MHz, Bruker Biospin Co., Billerica, MA).

2.3. Surface modification with the silanated MPCSi and SBSi

$TiAl_6V_4$ was polished and cleaned ultrasonically three times for 5 min each with ethanol and acetone after samples were cut to a predetermined size (1 cm × 2.5 cm) from a $TiAl_6V_4$ sheet. Titanium

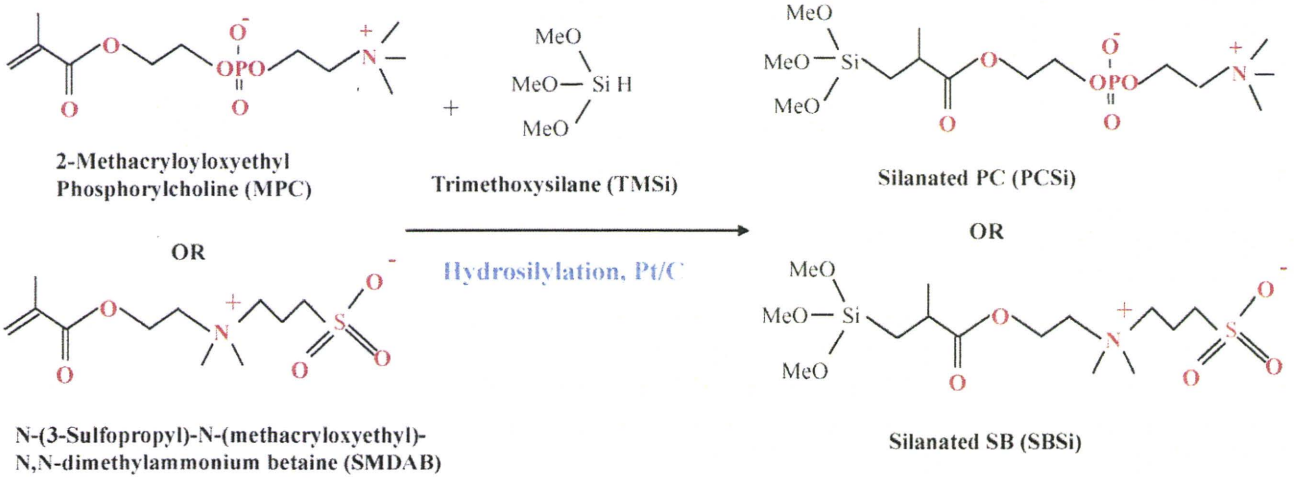

Fig. 1. Synthetic scheme for zwitterionic surface modifiers (PCSi or SBSi).

surfaces were passivated with a 35% nitric acid solution for 1 h and rinsed with distilled water for 24 h. Then, silanized titanium surfaces with the PCSi or SBSi were prepared by a hydrous liquid phase deposition method. The synthesized PCSi or SBSi was diluted at 3% concentration in MeOH and stirred for 30 min after adding the amount of necessary distilled water and HCl (0.05 M) to hydrolyze the methoxy groups of the PCSi or SBSi modifiers under acidic conditions (pH 4–5). Then the $TiAl_6V_4$ sample was immersed in the activated PCSi or SBSi solution and stirred for 30 min to adsorb the activated PCSi or SBSi on the titanium surface via weak hydrogen bonding. After that, the sample surfaces were dried in an oven for 1 h at 110 °C to silanize the surfaces with the PCSi or SBSi through covalent bonding. Samples treated in this manner were referred to as Ti-PCSi or Ti-SBSi. TMSi modified $TiAl_6V_4$ samples (Ti-TMSi) were also prepared by the same silanization reaction as a control. The modified samples were rinsed by stirring in deionized water for 24 h before using.

2.4. Surface characterization

The surface composition of the modified and unmodified $TiAl_6V_4$ samples was analyzed by X-ray photoelectron spectroscopy (XPS) using a Surface Science Instruments S-probe spectrometer at the University of Washington (Seattle, WA). The surface composition on a given sample was averaged from three composition spots. The mean value for three different samples was determined. The modified $TiAl_6V_4$ surfaces were also analyzed with an attenuated total reflection-Fourier transform infrared spectroscopy (ATR-FTIR, Shimadzu, Columbia, MD). The spectra were collected with 1024 scans at a resolution of 4 cm^{-1}. The static contact angle of water on the surfaces of unmodified and modified titanium samples was measured at room temperature using a contact angle goniometer (VCA optima, AST Product Inc., Billerica, MA) by placing 1 μL of distilled water on the surfaces. The contact angle was also measured after 4 weeks in the surface modified samples that underwent continuous stirring under deionized water to test the long-term stability of the surface modification. The $TiAl_6V_4$ surfaces were stained with rhodamine 6G (Sigma–Aldrich, St. Louis, MO) by immersing in rhodamine 6G aqueous solution (0.2 mg/mL) for 30 s, followed by washing in distilled water for 30 s and drying [28,29]. The surfaces were observed with fluorescence microscopy (ZEISS, Carl Zeiss, Inc. Thornwood, NY) and obtained images were analyzed with an Image-J program (National Institutes of Health, Washington, DC).

2.5. Surface protein adsorption

Surface protein adsorption on modified and unmodified $TiAl_6V_4$ samples was assessed by a micro-bicinchoninic acid (BCA) assay [30]. Ovine fibrinogen (Sigma–Aldrich) was prepared in phosphate buffer solution (PBS; BD Biosciences, San Jose, CA) at a concentration of 0.03 g/dL. The samples were immersed in the fibrinogen solution at 37 °C for 3 h followed by washing with 50 mL PBS. A protein analysis kit (Quantipro-Micro BCA kit, Sigma–Aldrich) based on the BCA method was used to quantify adsorbed fibrinogen. The mean value of fibrinogen adsorption from five independent samples, each measured in triplicate, was determined.

2.6. Blood collection and blood contact test

NIH guidelines for the care and use of laboratory animals were observed. Whole blood was collected from healthy ovines by jugular venipuncture using an 18 gauge 1.5″ needle after discarding the first 3 mL, and 2.7 mL was then immediately added to monovette tubes containing 0.3 mL of 0.106 M trisodium citrate (Sarstedt, Newton, NC). Whole ovine blood was also collected by jugular venipuncture directly into a syringe containing heparin (3.0 or 6.0 U/mL) after discarding the first 3 mL for blood contacting experiments. Then, modified titanium and unmodified $TiAl_6V_4$ samples were placed into Vacutainer® blood collection tubes without additives (BD Biosciences, Franklin Lakes, NJ), filled with citrate or heparinized ovine blood and incubated at 37 °C on a hematology mixer (Fisher Scientific, Pittsburgh, PA). Although some anticoagulation is necessary to perform the blood contact testing, citrate and heparin were both used to provide a comparison between stronger (citrate) and weaker (heparin) inhibitors of platelet deposition.

2.7. Scanning electron microscopy of platelet adhesion and morphology

After contact with citrated or heparinized ovine blood, surfaces were rinsed with PBS and immersed in a 2.5% glutaraldehyde solution for 2 h at 4 °C to fix the surface adherent platelets, and treated for 1 h in 1% (w/v) OsO_4. The samples were serially dehydrated with increasing ethanol solutions and sputter coated with gold/palladium. Each sample surface was observed by scanning electron microscopy (SEM; JSM-6330F, JEOL USA, Inc., Peabody, MA).

2.8. Quantification of platelet adhesion and activation

Modified and unmodified titanium samples were incubated with heparinized ovine blood for 2 h at 37 °C with continuous rocking as above. The surfaces were rinsed thoroughly after blood contact with 50 mL of PBS and immersed in 1 mL of 2% Triton X-100 solution (Sigma) for 20 min to lyse surface adherent platelets. The number of deposited platelets on each sample was then quantified by a lactate dehydrogenase (LDH) assay [31] with an LDH Cytotoxicity Detection Kit (Takara Bio, Tokyo, Japan). Calibration of spectrophotometer absorbance results to platelet numbers was accomplished using a calibration curve generated from known dilutions of ovine platelet rich plasma in the lysing solution. The

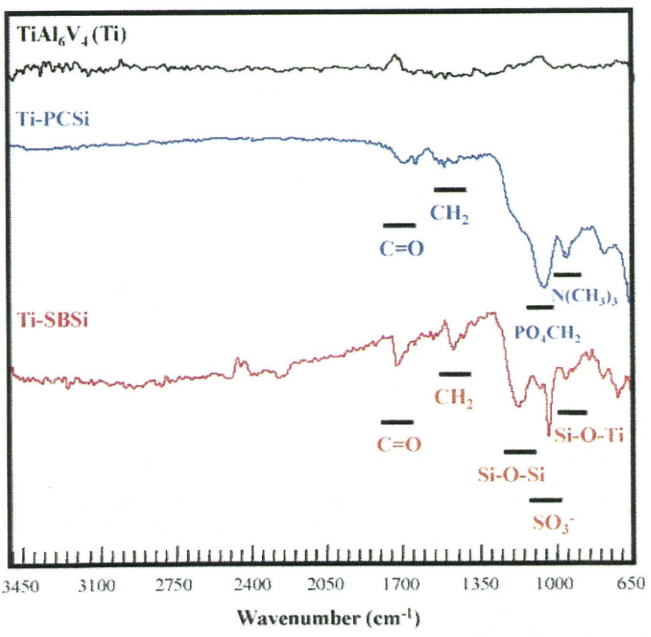

Fig. 2. Attenuated total reflectance (ATR)-FTIR spectra on the unmodified titanium ($TiAl_6V_4$ (Ti)), Ti-PCSi and Ti-SBSi.

Table 1
Atomic percentage at listed binding energy (eV) as determined by X-ray photoelectron spectroscopy.

	C 1s at 285 eV	O 1s at 532 eV	Ti 2p at 455 eV	Al 2p at 74 eV	Si 2p at 106 eV	N 1s at 403 eV	P 2p at 133 eV	S 2p at 168 eV
$TiAl_6V_4$ (Ti)	42.0 (±8.0)	41.1 (±5.2)	9.5 (±1.1)	4.3 (±3.1)	1.0 (±1.0)	1.0 (±0.5)	0.1 (±0.2)	0.0 (±0.0)
Ti-TMSi	44.8 (±12.9)	33.3 (±7.7)	2.3(±1.2)	2.7 (±1.5)	13.1 (±2.7)*	0.8 (±0.7)	0.0 (±0.0)	0.0 (±0.0)
Ti-PCSi	32.3 (±4.9)	47.4 (±3.9)	0.3 (±0.5)	0.5 (±0.8)	16.2 (±3.7)*	1.7 (±0.4)*	1.5 (±0.3)*	0.0 (±0.0)
Ti-SBSi	37.0 (±8.2)	40.3 (±6.8)	0.0 (±0.0)	1.2 (±2.1)	17.6 (±4.9)*	2.0 (±0.7)	0.0 (±0.0)	2.0 (±0.9)*

$N = 7$, ±standard deviation for Ti. $N = 3$, ±standard deviation for other samples.
* $p<0.05$ vs. Ti surfaces.

percentage of activated ovine platelets in the bulk phase of the blood contacting the surface samples was quantified by a flow cytometric assay using fluorescein conjugated Annexin V protein [32]. Activation levels from five independent samples were averaged for each surface type after subtracting the level of activation found for tubes filled with ovine blood that were rocked in the absence of a metallic surface specimen.

2.9. Statistical analyses

Data are presented as means with standard deviation. Statistical significance between sample groups was determined using ANOVA followed by post-hoc Newman–Keuls testing of specific differences. Statistical significance was considered to exist at $p < 0.05$.

3. Results

3.1. Surface modification and characterization of the modified $TiAl_6V_4$ with silanated zwitterionic modifier PCSi or SBSi

To achieve one-step surface modification of $TiAl_6V_4$ with non-specific protein adsorption, silanated zwitterionic modifier PCSi or SBSi were synthesized by hydrosilylation between trimethoxysilane and MPC or SMDAB. The hydrosilylation in this study occurred on Si–H to alkene group in the methacryloyl group of MPC and SMDAB in the presence of a platinum catalyst. The chemical structure of the synthesized PCSi and SBSi was confirmed by ^1H NMR. For PCSi (in deuterated ethanol) the peaks were: δ (ppm) 1.07–1.10 ($SiCH_2CHCH_3$, 2H), 1.15–1.20 ($SiCH_2CHCH_3$, 1H),

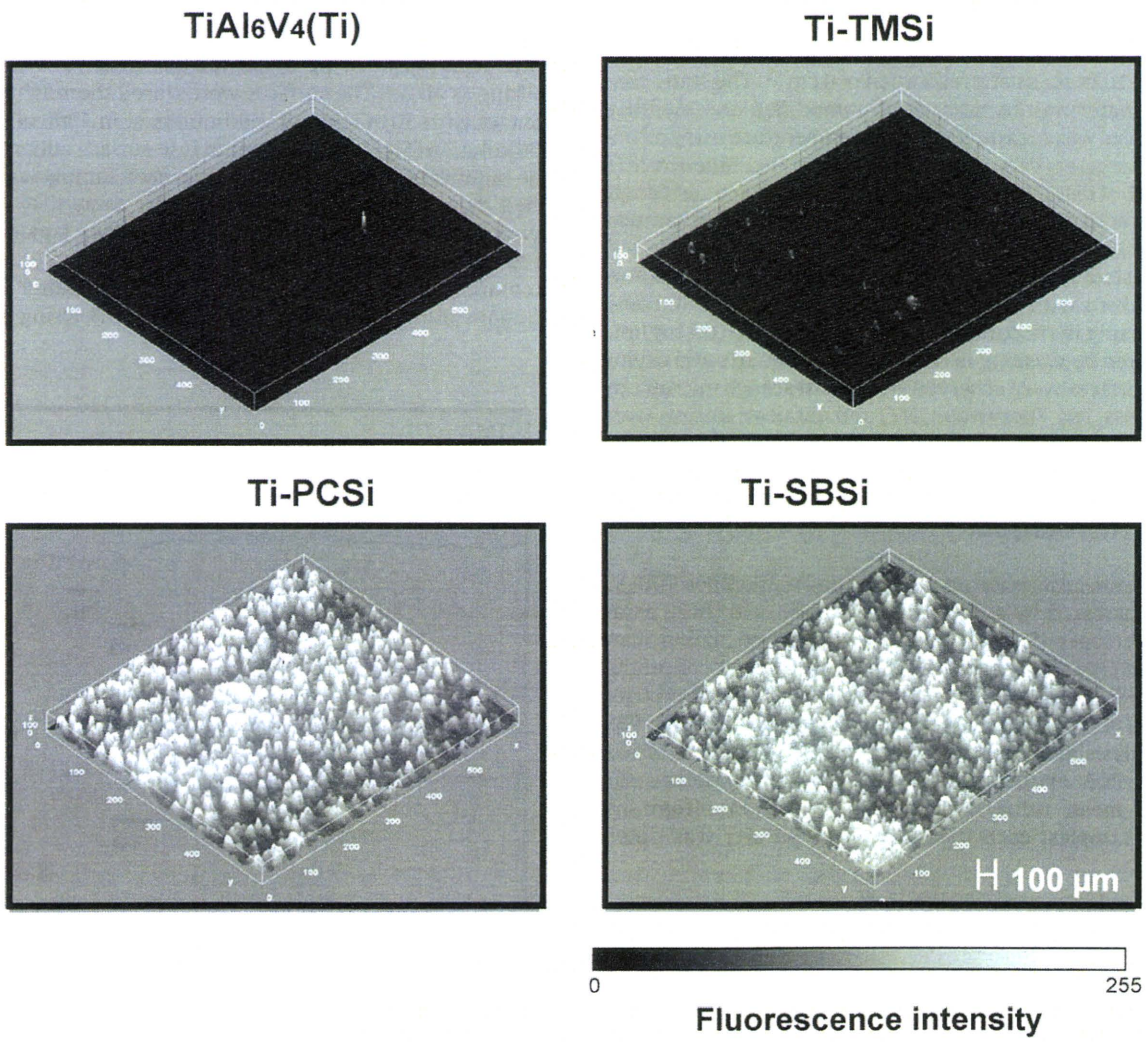

Fig. 3. Fluorescent micrograph images of unmodified $TiAl_6V_4$ (Ti), Ti-TMSi, Ti-PCSi and Ti-SBSi observed after staining with rhodamine 6G and digital image processing to create a 3D plot where the *z*-dimension is proportional to pixel intensity.

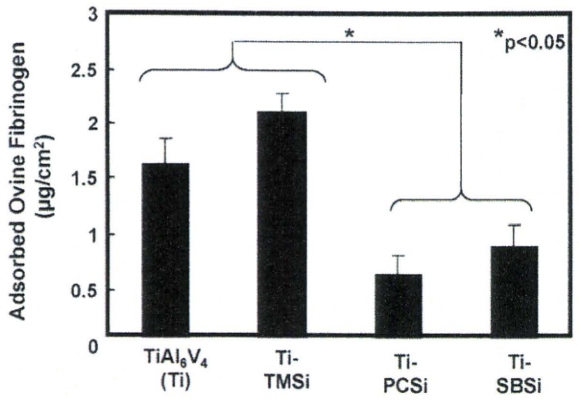

Fig. 4. Ovine fibrinogen adsorption from buffer at 37 °C for 3 h onto surfaces of control tissue culture polystyrene, unmodified and modified $TiAl_6V_4$ samples as determined by micro-BCA assay ($n = 5$).

1.90–2.11 ($SiCH_2CHCH_3$, 3H), 3.21–3.26 ($N(CH_3)_3$, 9H), 3.42–3.53 ($Si(OCH_3)_3$, 9H), 3.79–3.83 ($CH_2N(CH_3)_3$ 2H), 3.96–4.01 (OCH_2, 2H), 4.05–4.15 ($CH_2PO_4CH_2$, 4H), and for SBSi (in deuterated ethanol) the peaks were: δ (ppm) 0.92–0.94 ($SiCH_2CHCH_3$, 2H), 1.17–1.29 ($SiCH_2CHCH_3$, 3H), 1.37 ($SiCH_2CHCH_3$, 1H), 2.18–2.28 (CH_2CH_2S, 2H), 2.82–2.86 (CH_2CH_2S, 2H), 3.22–3.28 ($N(CH_3)_2$, 6H), 3.28–3.38 ($Si(OCH_3)_3$, 9H), 3.69–3.83 ($CH_2N(CH_3)_2CH_2$, 4H) and 4.54–4.60 (OCH_2, 2H).

The surface composition analyzed by XPS is also shown in Table 1. The surfaces modified with TMSi which were prepared as a control showed a decrease in Ti composition and increased Si composition in comparison with unmodified $TiAl_6V_4$ (Ti) ($p < 0.05$). The data also support the successful modification of $TiAl_6V_4$ surfaces with the PCSi or SBSi based on an increased phosphorus composition ($P = 1.5 \pm 0.2\%$) on the surface of Ti-PCSi and an increased sulfur composition ($S = 2.5 \pm 1.1\%$) on the surface of Ti-SBSi in comparison to unmodified $TiAl_6V_4$ (Ti) and Ti-TMSi ($p < 0.05$). An attenuated total reflection FTIR spectrum for each surface is shown in Fig. 2. On the surface of Ti-PCSi and SBSi, there are new absorbance peaks at 1723 cm^{-1} (C=O stretching vibration), 1480–1300 cm^{-1} (CH_2, CH_3 bending), 1250–1020 cm^{-1} (Si–O–Si asymmetric stretching vibration), 1150–1050 cm^{-1} ($PO_4CH_2^-$ stretching vibration), 1172, 1040 cm^{-1} (SO_3^- vibration), 970 cm^{-1} ($N(CH_3)_3$ vibration), 925–950 cm^{-1} (Si–O–Ti siloxane bond to titanium) [33,34].

Fluorescent micrograph images of unmodified $TiAl_6V_4$ (Ti), Ti-TMSi, Ti-MPCSi and Ti-SBSi observed after staining with rhodamine 6G and generating 3D plots of the fluorescence intensity are seen in Fig. 3. Both the PCSi modified surface (Ti-PCSi) and the Ti-SBSi stained strongly with the rhodamine and coverage was relatively uniform. Unmodified $TiAl_6V_4$ (Ti) and Ti-TMSi control surfaces did not stain positively and yielded dark images.

Table 2 shows the surface contact angle before and after surface modification. The surface contact angles significantly decreased on both the Ti-PCSi and Ti-SBSi in comparison with $TiAl_6V_4$ (Ti) and Ti-TMSi attributable to the presence of the hydrophilic PC and SB groups on the surfaces. The contact angles did not significantly change after continuous rinsing with deionized water over a 4 week period.

The amount of adsorbed ovine fibrinogen on the unmodified and modified titanium surfaces is shown in Fig. 4. Both the Ti-PCSi and Ti-SBSi showed a significant decrease in adsorbed fibrinogen relative to Ti and Ti-TMSi surfaces.

3.2. *In vitro surface blood compatibility of the modified $TiAl_6V_4$*

Electron micrographs of platelet deposition from citrated ovine blood for 3 h at 37 °C for unmodified $TiAl_6V_4$ (Ti) and modi-

Table 2
Contact angle with distilled water on the unmodified and modified titanium samples.

	$TiAl_6V_4$ (Ti)	Ti-TMSi	Ti-PCSi	Ti-SBSi	Ti-PCSi after 4 weeks of rinsing	Ti-SBSi after 4 weeks of rinsing
Contact angle (°)	53.7 (±4.1)	95.2 (±4.1)	16.4 (±3.9)*	21.8 (±5.5)*	22.9 (±3.2)*	24.9 (±4.4)*

$N = 3$, ±standard deviation.
* $p < 0.05$ vs. Ti and Ti-TMSi surfaces.

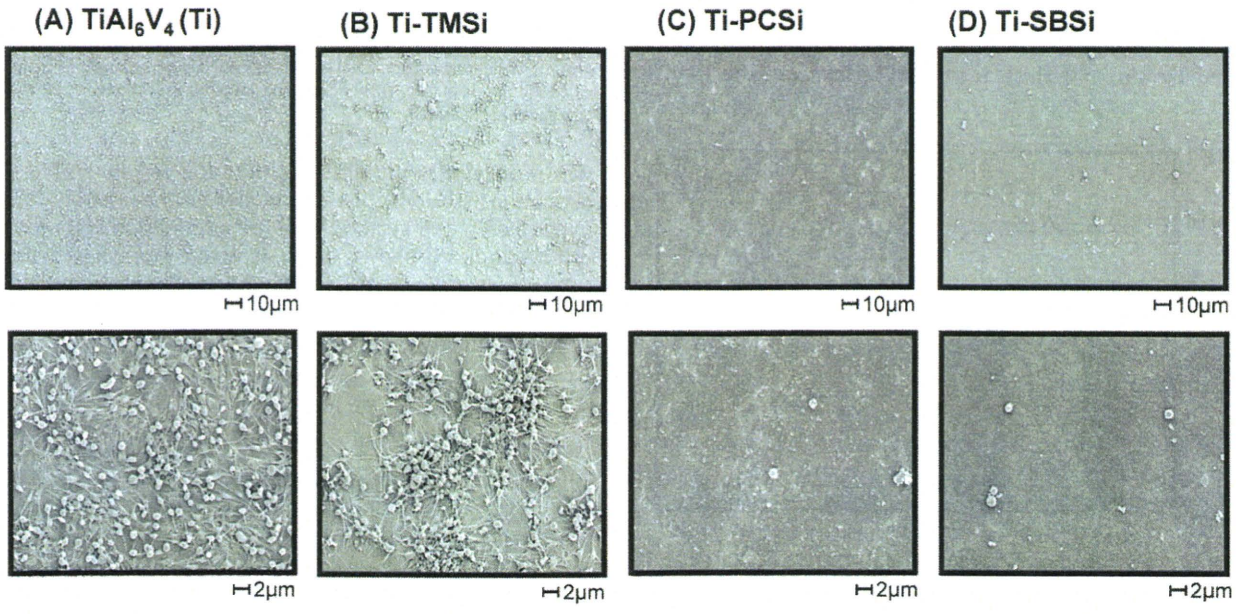

Fig. 5. Low (top row) and high (bottom row) magnification scanning electron micrographs of $TiAl_6V_4$ (Ti), Ti-TMSi, Ti-PCSi and Ti-SBSi samples after contact with fresh ovine blood (citrated) under mixing for 3 h at 37 °C.

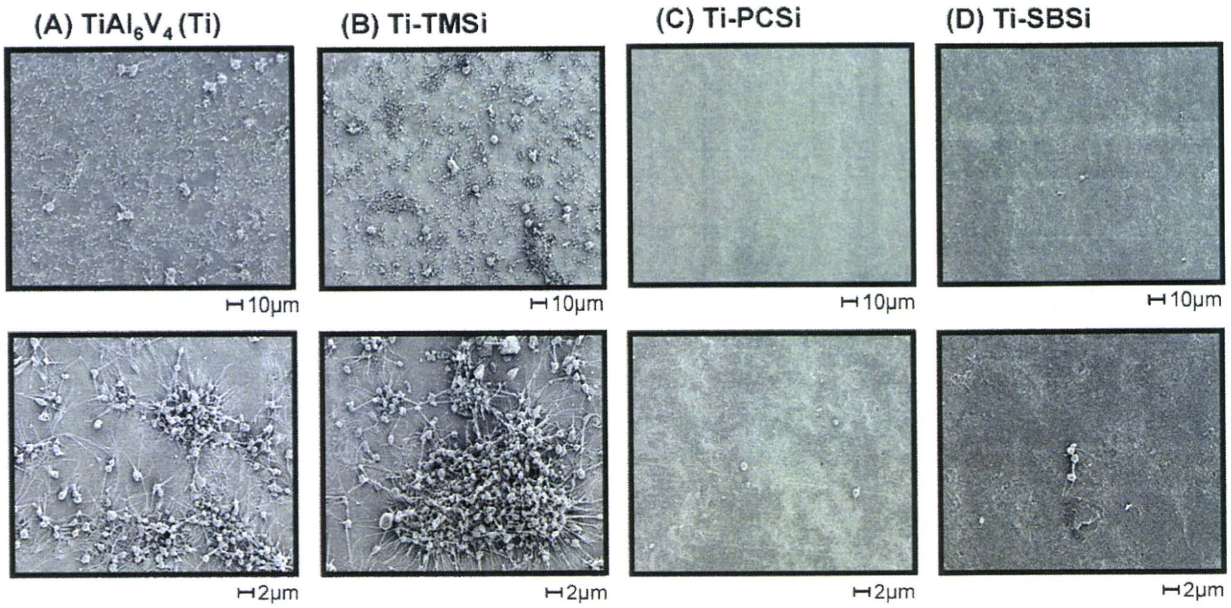

Fig. 6. Low (top row) and high (bottom row) magnification scanning electron micrographs of $TiAl_6V_4$ (Ti), Ti-TMSi, Ti-PCSi and Ti-SBSi samples after contact with fresh ovine blood (with heparin at 3 U/mL) under mixing for 2 h at 37°C.

fied titanium samples (Ti-TMSi, Ti-PCSi and Ti-SBSi) are shown in Fig. 5. There were many adhered platelets on the unmodified Ti and Ti-TMSi surfaces and some platelet aggregation was seen. The deposited platelets exhibited an activated morphology, as demonstrated by extended pseudopodia and surface spreading. In contrast, platelet deposition was sparse on the Ti-PCSi and Ti-SBSi surfaces and those platelets found were in a discoid morphology without signs of surface activation. Platelet adhesion and morphology was also observed after contact with heparinized ovine blood (3 U/mL) for 2 h at 37 °C (Fig. 6). Platelet deposition and surface aggregation appeared to increase on the Ti and Ti-TMSi surfaces with the heparinized blood when compared to surfaces in contact with citrated blood. The marked decrease in platelet deposition on the Ti-PCSi and Ti-SBSi surfaces compared to the Ti and Ti-TMSi samples was again observed with the heparinized blood.

The number of deposited platelets as quantified by the lactate dehydrogenase (LDH) assay after heparinized ovine blood contact is shown in Fig. 7. The Ti-PCSi and Ti-SBSi modified surfaces showed large decreases in the number of deposited platelets relative to unmodified $TiAl_6V_4$ and Ti-TMSi ($p < 0.01$). However, the Ti-PCSi

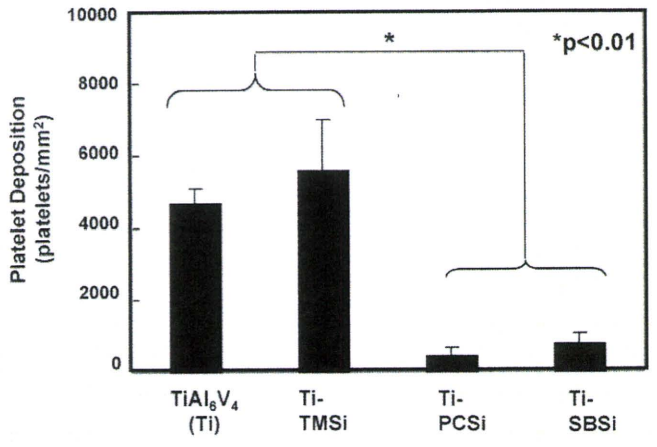

Fig. 7. Platelet deposition onto surfaces after contact with ovine blood (with heparin at 6 U/mL) for 2 h under mixing as determined by lactate dehydrogenase (LDH) assay ($n = 5$).

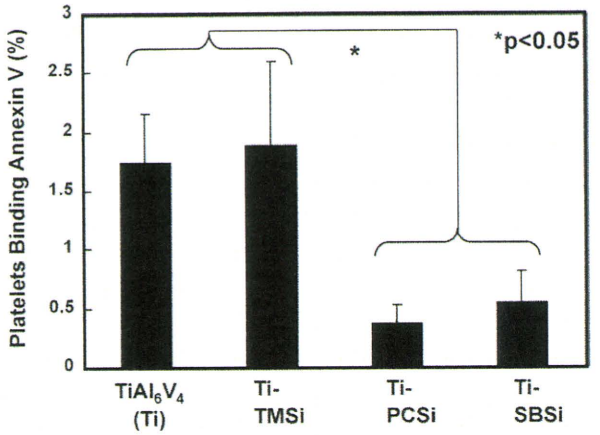

Fig. 8. Quantification of activated platelets in the bulk phase of ovine blood after surface contact under continuous rocking. Platelet activation was quantified by flow cytometric measurement of Annexin V binding onto platelets ($n = 5$). The background platelet activation level was determined from a rocked tube into which no test surface was placed. This background value was subtracted from all tests where a surface was included.

was not significantly different than the Ti-SBSi surfaces. Platelet activation in the bulk phase, as evidenced by Annexin V binding, for ovine blood after contact with the unmodified and modified titanium samples is shown in Fig. 8, where platelet activation levels following contact with Ti-PCSi and Ti-SBSi samples were significantly lower than that for unmodified $TiAl_6V_4$ (Ti) and Ti-TMSi control samples.

4. Discussion

There is increasing interest in zwitterionic moieties including carboxybetaine (CB), sulfobetaine (SB) and phosphobetaine (PC group-bearing polymer) to design biocompatible polymeric materials since surfaces modified with these moieties are less supportive of untoward cell adhesion or enzymatic activation based on their minimization of protein adsorption [35]. Kitano et al. [36–38] showed common effects of zwitterionic group-bearing polymer surfaces on the structure of surrounding water in that PC, SB or

CB groups did not disturb the hydrogen-bonding network structure of water. It was further suggested that the resistance of these surfaces to protein adsorption related to the local water structure [39].

To initiate chemical modification of a polymeric biomaterial surface, there are many approaches that have been pursued, including direct grafting with a zwitterionic group containing monomer [24,25,40–42] or the use of alkoxysilane compounds which have PC, SB or CB groups such as PCSi or SBSi as surface modifiers [43,44]. However, previous studies have required a complicated synthesis route to generate the appropriate PC or SB groups and attach these onto the surface. In this report we simply prepared PCSi and SBSi as titanium alloy surface modifiers by a hydrosilylation reaction using MPC or SMDAB. This reaction between a hydride-siloxane (Si–H) and vinyl (C=C) compounds with a catalyst such as Pt/C is relatively simple and is widely used in the silicone industry to prepare monomers, silicone-carbon compounds and crosslinkable polymers [45]. In this study, there was concern about the lower reactivity of methacrylate groups in comparison with vinyl groups [46], however the hydrosilylation of methacrylate groups was confirmed at almost 100% completion under mildly increased temperature (40 °C), provided the Si–H and catalyst were in excess and the reaction time was sufficient. The NMR analysis of synthesized PCSi and SBSi did not show any double bond peaks at 5.2–5.5 and 6.0–6.2 ppm, which would be associated with unreacted monomers. The purified PCSi and SBSi product could be collected and stored without aggregation of the siloxane compounds by keeping anhydrous conditions during the synthesis process.

West et al. [26] evaluated two copolymers containing SB or PC moieties for use as potential biocompatible coatings. They showed that both SB and PC group-bearing polymer coatings reduced cell adhesion (bacterial adhesion, human macrophages, and granulocytes) with respect to the uncoated materials, and that PC group-bearing copolymer coatings were superior to the SB-based copolymer coatings in reducing cellular adhesion. In this study, we prepared a titanium alloy surface that was modified with PC or SB groups using silanated PC or SB modifiers (PCSi or SBSi) and the modified surfaces (Ti-PCSi or Ti-SBSi) were compared in terms of fibrinogen adsorption, platelet deposition and platelet activation. Both the Ti-PCSi and Ti-SBSi surfaces experienced significantly reduced fibrinogen adsorption, platelet deposition and bulk phase platelet activation relative to unmodified Ti and Ti-TMSi control samples. Although there was a trend toward lower average values for platelet deposition, fibrinogen adsorption, and platelet activation for the Ti-PCSi relative to the Ti-SBSi, none of these differences were found to be statistically significant.

The PCSi and SBSi modified surfaces were prepared by hydrous liquid phase deposition so that the three methoxy groups of the PCSi and SBSi were changed to hydroxyl groups and the hydrolyzed PCSi and SBSi were deposited in the bulk state. The hydrolyzed modifiers had three reactive sites (hydroxyl groups) and could react with each other as well as the desired hydroxyl groups of the titanium surface. This alternative reaction by the PCSi and SBSi with tri-hydroxyl groups could result in non-uniform surfaces (bulk deposition of the PCSi and SBSi) as was seen to some extent with rhodamine staining. A relatively large variation was also observed in the SBSi composition of Ti-SBSi samples as evidenced by the XPS results (Table 1). The surface uniformity might be better controlled by changing the PCSi or SBSi modifiers concentration, silanization conditions or the modifier reactivity. A more uniform surface could be obtained by an anhydrous liquid phase deposition method where the PCSi and SBSi could deposit on the titanium surface in anhydrous toluene with a catalyst at room temperature by stirring for 24 h without hydrolysis of the methoxy groups. Toward this end we also prepared a PCSi or SBSi monolayer deposited surfaces with these surface modifiers and mono-functional silanated PCSi and SBSi modifiers from 1-chlorodimethylsilane with the same hydrosilylation reaction, and then reacted with the titanium surface to prepare a more uniform surface. The mono-functional silanated PCSi and SBSi modification on a $TiAl_6V_4$ surface also showed a significant decrease in platelet adhesion and activation compared to the control surface. However, it was difficult to prepare a highly covered monolayer with these mono-functional modifiers and the modified surfaces did not show improved performance in decreasing platelet deposition and activation relative to the bulk deposited PCSi or SBSi modified surfaces (data not shown). This may have been due to difficulty in achieving monolayer coverage with PCSi and SBSi modifiers because of imperfect monolayer availability of hydroxyl groups on the alloy substrate. In this study, we did not apply a water plasma treatment before the PCSi and SBSi modification, though we demonstrated that water plasma treatment could increase the surface reactivity of the titanium alloy in previous studies [20,21]. Better monolayer deposition may have resulted from further surface treatment, such as water plasma exposure or other chemical pretreatments, to increase hydroxyl group numbers on the surface before silanization with the PCSi and SBSi modifiers. However, the bulk deposition of PCSi or SBSi prepared under the hydrous liquid phase deposition conditions may have increased the coverage and modification density of the PC or SB groups on the surface without needing to increase the reactive hydroxyl groups on the bare titanium surface.

Previously we reported that PC group-bearing polymers could be attached onto a titanium alloy surface by immobilizing an MPC copolymer (poly(MPC-co-methacryl acid) (PMA)) or by plasma induced MPC grafting polymerization after the titanium surface was pre-modified with a functional silane coupling agent [20,21]. Those surfaces showed significant improvement over non-modified surfaces in terms of decreased platelet deposition and bulk phase platelet activation. However, those techniques required multiple steps to pre-functionalize the surface in order to immobilize or graft the PC group-bearing polymer onto the titanium surface. There was no significant difference in terms of the inhibition of platelet deposition and activation when comparing the current one-step procedure with these previous titanium surfaces modified with PC group-bearing polymers [20,21]. The simpler and equally effective surface modification method using a small silanated PC molecule (PCSi) thus is more attractive in that this coating could be applied in a direct manner under mild conditions and could be readily applied to the assembled, complex geometries of a cardiovascular device such as a rotary blood pump [47].

While in our study the SB-based surface modification did not exhibit a significantly greater biological effect than that found with PCSi, and in fact trended to less of an effect, further investigation of this surface modifier is warranted due to its cost being orders of magnitude lower than for the PC-containing modifier. Earlier studies by Bernards et al. [48] prepared nonfouling polymer brushes composed of varying mixtures of positively [$-N^+$] and negatively [$-SO_3^-$] charged monomers by surface initiated atom transfer polymerization (ATRP) on a gold-coated surface. Their results demonstrated that the polymer brush surface coating composed of oppositely charged monomers exhibited low protein adsorption. Their best nonfouling surface coating was copolymer brushes formed from a 1:1 homogeneous reaction mixture of two oppositely charged monomers. Furthermore, Zhang et al. [49] prepared a "superlow" fouling surface on glass slides by grafting SB- or CB-bearing polymers by surface initiated ATRP. Better controlled surface modification techniques such as offered by surface initiated ATRP might maximize the surface modification effect of sulfobetaine and result in further improvements in surface blood biocompatibility.

Some limitations of the current report should be noted. First, in this study, we polished a raw titanium alloy sheet by hand with

diamond pastes of 3, 1, 0.25 and 0.1 μm size. While this level of polish was utilized to mimic the materials being employed industrially for a blood pump, the roughness of the polished, unmodified titanium surface was of a scale that additional texture added from the surface modification would not likely be detectable by AFM and ellipsometry, as noted in our previous study [21]. A more complete surface modification and more extensive surface analysis would be possible if a more highly polished surface were to be employed, although this would not likely match the types of surfaces utilized with many devices being employed clinically. Second, the amount of adsorbed protein estimated by the micro-BCA method (Fig. 4) was higher than for previous reports where the zwitterionic PC or SB groups have been attached in monolayer to more idealized surfaces [27,48]. In these reports more accurate quantification methods, such as a quartz crystal microbalance (QCM) and surface plasmon resonance (SPR), were employed. In this study, the micro-BCA method was used to provide for a relatively simple comparison between unmodified and variably modified surfaces and the levels of fibrinogen adsorption measured were generally consistent with previous reports employing the micro-BCA method [10,20]. Finally, the efficacy of the generated surfaces was evaluated in an in vitro setting, with ovine blood, for a relatively limited period of blood contact. While blood mixing was present, the hemodynamic environment would not match either the high flow regimes experienced in, for instance, a rotary blood pump, nor would there be the non-ideal flow conditions that one might experience in a crevice formed by connecting metallic parts or in regions of flow recirculation behind impeller blades [47]. Next steps for surface evaluation would involve the coating of cardiovascular devices for extended blood contact under relevant hemodynamic conditions with in vitro perfusion loops, and with testing in appropriate large animal models. A challenge with such experiments is the expense of generating multiple devices for comparative testing and the maintenance of implanted animals, although such experiments are possible and have shown the potential benefits of MPC-based coatings on blood pump biocompatibility in vivo [15].

5. Conclusions

Silanated zwitterionic surface modifiers (PCSi or SBSi) were successfully prepared from trimethoxysilane and MPC or SMDAB by a hydrosilylation reaction. Non-thrombogenic interfaces were simply achieved on a $TiAl_6V_4$ surfaces by the covalent attachment of PCSi or SBSi onto the surface in a single step modification reaction. Platelet deposition and bulk phase platelet activation were significantly decreased on PCSi or SBSi modified $TiAl_6V_4$ surfaces in comparison with unmodified and trimethoxysilane modified control surfaces. This single step modification with PCSi or SBSi modifiers offers promise for improving the surface hemocompatibility of blood contacting devices utilizing $TiAl_6V_4$ and is attractive for its ease of application to potentially complex device surfaces.

Acknowledgements

This research was supported by the NSF Engineering Research Center for Revolutionizing Metallic Biomaterials (Award #0812348) and NIH contract # HHSN268200448192C. Mr. Johnson was supported by a United Negro College Fund MERCK Graduate Science Research Dissertation Fellowship. Mr. Woolley was supported by NIH training grant # T32-HL076124.

References

[1] L.R. McBride, K.S. Naunheim, A.C. Fiore, D.A. Moroney, M.T. Swartz, Ann. Thorac. Surg. 67 (1999) 1233.
[2] X. Liu, P.K. Chu, C. Ding, Mater. Sci. Eng. R 47 (2004) 49.
[3] M.A. Simon, J. Watson, J.T. Baldwin, W.R. Wagner, H.S. Borovetz, Annu. Rev. Biomed. Eng. 10 (2008) 59.
[4] C. Hansi, A. Arab, A. Rzany, I. Ahrens, C. Bode, C. Hehrlein, Catheter. Cardiovasc. Interv. 73 (2009) 488.
[5] D.C. Sin, H.L. Kei, X. Miao, Expert Rev. Med. Devices 6 (2009) 51.
[6] K. Ishihara, T. Ueda, N. Nakabayashi, Polym. J. 22 (1990) 355.
[7] K. Ishihara, Trends Polym Sci. 5 (1997) 401.
[8] A.L. Lewis, Colloids Surf. B: Biointerfaces 18 (2000) 261.
[9] K. Ishihara, Sci. Technol. Adv. Mater. 1 (2000) 131.
[10] S.H. Ye, J. Watanabe, Y. Iwasaki, K. Ishihara, Biomaterials 24 (2003) 4143.
[11] K. Ishihara, M. Takai, J. R. Soc. Interface 6 (2009) S279.
[12] D.M. Whelan, W.J. Giessen, S.C. Krabbendam, E.A. Vliet, P.D. Verdouw, P.W. Serruys, H.M.M. Beusekom, Heart 83 (2000) 338.
[13] M. Galli, L. Sommariva, F. Prati, S. Zerboni, A. Politi, R. Bonattie, S. Mameli, E. Butti, A. Pagano, G. Ferrari, Catheter. Cardiovasc. Interv. 53 (2001) 182.
[14] S. Kihara, K. Yamazaki, P. Litwak, M.V. Kameneva, H. Ushiyama, T. Tokuno, D.C. Borzelleca, M. Umezu, J. Tomioka, O. Tagusari, T. Akimoto, H. Koyanagi, H. Kurosawa, R.L. Kormos, B.P. Griffith, Artif. Organs 27 (2003) 188.
[15] T.A. Snyder, H. Tsukui, S. Kihara, T. Akimoto, K.N. Litwak, M.V. Kameneva, K. Yamazaki, W.R. Wagner, J. Biomed. Mater. Res. 81 (2007) 85.
[16] A. Shirakura, M. Nakaya, Y. Koga, H. Kodama, T. Hasebe, T. Suzuki, Thin Solid Films 494 (2006) 84.
[17] D. Cruz, R. Karlsberg, Y. Takano, M. Rosove, D. Vora, J. Tobis. Catheter. Cardiovasc. Interv. 58 (2003) 80.
[18] J.A. Bittl, Catheter. Cardiovasc. Interv. 58 (2003) 84.
[19] L. Mureebe, J. Graham, R. Bush, D. Silver, Ann. Vasc. Surg. 21 (2007) 719.
[20] S.H. Ye, C.A. Johnson Jr., J.R. Woolley, T.A. Snyder, L.J. Gamble, W.R. Wagner, J. Biomed. Mater. Res. A 91 (2009) 18.
[21] S.H. Ye, C.A. Johnson Jr., J.R. Woolley, H.I. Oh, L.J. Gamble, K. Ishihara, W.R. Wagner, Colloids Surf. B: Biointerfaces 74 (2009) 96.
[22] H.S. Borovetz, S. Badylak, J.R. Boston, C. Johnson, R. Kormos, M.V. Kameneva, M. Simaan, T.A. Snyder, H. Tsukui, W.R. Wagner, J. Woolley, J. Antaki, C. Diao, S. Vandenberghe, B. Keller, V. Morell, P. Wearden, S. Webber, J. Gardiner, C.M. Li, D. Paden, B. Paden, S. Snyder, J. Wu, G. Bearnson, J.A. Hawkins, G. Jacobs, J. Kirk, P. Khanwilkar, P.C. Kouretas, J. Long, R.E. Shaddy, Cell Transplant. 15 (Suppl. 1) (2006) 69 (review).
[23] R.E. Holmlin, X. Chen, R.G. Chapman, S. Takayama, G.M. Whitesides, Langmuir 17 (2001) 2841.
[24] Y.L. Yuan, F. Ai, J. Zhang, X.B. Zang, J. Shen, S.C. Lin, J. Biomater. Sci. Polymer Ed. 13 (2002) 1081.
[25] J. Zhang, J. Yuan, Y.L. Yuan, X.P. Zang, J. Shen, S.C. Lin, Biomaterials 24 (2003) 4223.
[26] S.L. West, J.P. Salvage, E.J. Lobb, S.P. Armes, N.C. Billingham, A.L. Lewis, G.W. Hanlon, A.W. Lloyd, Biomaterials 25 (2004) 1195.
[27] H. Kitano, A. Kawasaki, H. Kawasaki, S. Morokoshi, J. Colloid Interface Sci. 282 (2005) 340.
[28] J.H. Wang, J.D. Bartlett, A.C. Dunn, S. Small, S.L. Willis, J. Driver, A.L. Lewis, J. Microsc. 217 (2005) 216.
[29] M. Kyomoto, Y. Iwasaki, T. Moro, T. Konno, F. Miyaji, H. Kawaguchi, Y. Takatori, K. Nakamura, K. Ishihara, Biomaterials 28 (2007) 3121.
[30] P.K. Smith, R.I. Krohn, G.T. Hermanson, A.K. Mallia, F.H. Gartner, M.D. Provenzano, E.K. Fujimoto, N.M. Goeke, B.J. Olson, D.C. Klenk, Anal. Biochem. 150 (1985) 76.
[31] Y. Tamada, E.A. Kulik, Y. Ikada, Biomaterials 16 (1995) 259.
[32] C.A. Johnson Jr., T.A. Snyder, J.R. Woolley, W.R. Wagner, Artif. Organs 32 (2008) 136.
[33] Y.L. Yuan, F. Ai, X.P. Zang, W. Zhang, J. Shen, S.C. Lin, Colloids Surf. B: Biointerfaces 35 (2004) 1.
[34] J.P. Matinlinna, S. Areva, L.V.J. Lassila, P.K. Vallittu, Surf. Interface Anal. 36 (2004) 1314.
[35] H. Chen, L. Yuan, W. Song, Z. Wu, D. Li, Prog. Polym. Sci. 33 (2008) 1059.
[36] H. Kitano, K. Sudo, K. Ichikawa, M. Ide, K. Ishihara, J. Phys. Chem. B 104 (2000) 11425.
[37] H. Kitano, M. Imai, T. Mori, M. Gemmei-Ide, Y. Yokoyama, K. Ishihara, Langmuir 19 (2003) 10260.
[38] H. Kitano, S. Tada, T. Mori, K. Takaha, M. Gemmei-Ide, M. Tanaka, M. Fukuda, Y. Yokoyama, Langmuir 21 (2005) 11932.
[39] K. Ishihara, H. Nomura, T. Mihara, K. Kurita, Y. Iwasaki, N. Nakabayashi, J. Biomed. Mater. Res. 39 (1998) 323.
[40] Z.K. Xu, Q.W. Dai, J. Wu, X.J. Huang, Q. Yang, Langmuir 20 (2004) 1481.
[41] X.J. Huang, Z.K. Xu, L.S. Wan, Z.G. Wang, J.L. Wang, Langmuir 21 (2005) 2941.
[42] P. Chevalllier, R. Janvier, D. Mantovani, G. Laroche, Macromol. Biosci. 5 (2005) 829.
[43] T. Miyazaki, Y. Koinuma, US Patent 5,936,703A (1999).
[44] Y.Z. Qiu, D.Y. Min, C. Ben, J. Shen, Q. Chen, S.C. Lin, Chin. J. Polym. Sci. 23 (2005) 611.
[45] L.N. Lewis, J. Stein, Y. Gao, R.E. Colborn, G. Hutchins, Platinum Met. Rev. 41 (1997) 66.
[46] S.J. Wang, X.D. Fan, J. Kong, J.R. Lu, Polymer 50 (2009) 3587.
[47] J. Wu, J.F. Antaki, W.R. Wagner, T.A. Snyder, B.E. Paden, H.S. Borovetz, ASAIO J. 51 (2005) 636.
[48] M.T. Bernards, G. Cheng, Z. Zhang, S. Chen, S. Jiang, Macromolecules 41 (2008) 4216.
[49] Z. Zhang, T. Chao, T. Chen, S. Jiang, Langmuir 22 (2006) 10072.

Biomaterials 31 (2010) 658–668

Contents lists available at ScienceDirect

Biomaterials

journal homepage: www.elsevier.com/locate/biomaterials

Lubricity and stability of poly(2-methacryloyloxyethyl phosphorylcholine) polymer layer on Co–Cr–Mo surface for hemi-arthroplasty to prevent degeneration of articular cartilage

Masayuki Kyomoto [a,c,f], Toru Moro [c,d], Ken-ichi Saiga [a,c,f], Fumiaki Miyaji [f], Hiroshi Kawaguchi [d], Yoshio Takatori [c,d], Kozo Nakamura [d], Kazuhiko Ishihara [a,b,e,*]

[a] Department of Materials Engineering, The University of Tokyo, 7-3-1 Hongo, Bunkyo-ku, Tokyo 113-8654, Japan
[b] Department of Bioengineering, School of Engineering, The University of Tokyo, 7-3-1 Hongo, Bunkyo-ku, Tokyo 113-8654, Japan
[c] Division of Science for Joint Reconstruction, Graduate School of Medicine, The University of Tokyo, 7-3-1 Hongo, Bunkyo-ku, Tokyo 113-8654, Japan
[d] Sensory & Motor System Medicine, Faculty of Medicine, The University of Tokyo, 7-3-1 Hongo, Bunkyo-ku, Tokyo 113-8654, Japan
[e] Center for NanoBio Integration, The University of Tokyo, 7-3-1 Hongo, Bunkyo-ku, Tokyo 113-8654, Japan
[f] Research Department, Japan Medical Materials Corporation, 3-3-31 Miyahara, Yodogawa-ku, Osaka 532-0003, Japan

ARTICLE INFO

Article history:
Received 30 July 2009
Accepted 22 September 2009
Available online 9 October 2009

Keywords:
Phosphorylcholine
Cobalt alloy
Hip replacement prosthesis
Surface modificaiton
Cartilage
Friction

ABSTRACT

Migration of the artificial femoral head to the inside of the pelvis due to the degeneration of acetabular cartilage has emerged as a serious issue in resurfacing or bipolar hemi-arthroplasty. Surface modification of cobalt–chromium–molybdenum alloy (Co–Cr–Mo) is one of the promising means of improving lubrication for preventing the migration of the artificial femoral head. In this study, we systematically investigated the surface properties, such as lubricity, biocompatibility, and stability of the various modification layers formed on the Co–Cr–Mo with the biocompatible 2-methacryloyloxyethyl phosphorylcholine (MPC) polymer by dip coating or grafting. The cartilage/poly(MPC) (PMPC)-grafted Co–Cr–Mo interface, which mimicked a natural joint, showed an extremely low friction coefficient of <0.01, as low as that of a natural cartilage interface. Moreover, the long-term stability in water was confirmed for the PMPC-grafted layer; no hydrolysis of the siloxane bond was observed throughout soaking in phosphate-buffered saline for 12 weeks. The PMPC-grafted Co–Cr–Mo femoral head for hemi-arthroplasty is a promising option for preserving acetabular cartilage and extending the duration before total hip arthroplasty.

1. Introduction

Resurfacing or bipolar hemi-arthroplasty for the treatments of osteoarthritis or osteonecrosis of hip of the young, active patient profile, and fractures of the femur neck of the typically aged patient profile, has long been advocated [1]. Consequently, resurfacing and bipolar hemi-arthroplasties can be possibly used as delaying tactics prior to revision surgeries of total hip arthroplasty. Most patients receive dramatic pain relief and rapid improvement in both their daily activities and quality of life due to advantages such as reduced blood loss, lower dislocation, ease of implantation, etc. However, migration of the artificial femoral head to the inside of the pelvis due to the degeneration of acetabular cartilage has emerged as a serious issue in the hemi-arthroplasties [2]. The longevity of the artificial femoral head after hemi-arthroplasty depends upon the quality of the acetabular cartilage or the lubrication conditions between the artificial femoral head and acetabular cartilage. Surface modifications of cobalt–chromium–molybdenum alloy (Co–Cr–Mo) for the artificial femoral head is one of the promising means of improving lubrication and preventing the degradation of acetabular cartilage, thereby preventing the migration of the artificial femoral head. Such surface modifications may improve hemi-arthroplasty survival, and liberate the restrictions for its application to younger, active patients.

Most frequently, surface modification with polymer is performed using either of the following methods: (1) surface-initiated graft polymerization, termed as the "grafting from" method, in which monomers are polymerized from initiators, and the polymeric molecules are grafted onto the substrate through covalent bonding; and (2) adsorption or immobilization of the polymer onto

* Corresponding author. Department of Materials Engineering, School of Engineering, The University of Tokyo, Hongo 7-3-1, Bunkyo-ku, Tokyo 113-8656, Japan. Tel.: +81 3 5841 7124; fax: +81 3 5841 8647.
E-mail address: ishihara@mpc.t.u-tokyo.ac.jp (K. Ishihara).

0142-9612/$ – see front matter © 2009 Elsevier Ltd. All rights reserved.
doi:10.1016/j.biomaterials.2009.09.083